THE IIOAB JOURNAL

VOLUME 11 : NO 4 : OCTOBER 2020 : ISSN 0976-3104

Institute of Integrative Omics and Applied Biotechnology Journal

Dear Esteemed Readers, Authors, and Colleagues,

I hope this letter finds you in good health and high spirits. It is my distinct pleasure to address you as the Editor-in-Chief of Integrative Omics and Applied Biotechnology (IIOAB) Journal, a multidisciplinary scientific journal that has always placed a profound emphasis on nurturing the involvement of young scientists and championing the significance of an interdisciplinary approach.

At Integrative Omics and Applied Biotechnology (IIOAB) Journal, we firmly believe in the transformative power of science and innovation, and we recognize that it is the vigor and enthusiasm of young minds that often drive the most groundbreaking discoveries. We actively encourage students, early-career researchers, and scientists to submit their work and engage in meaningful discourse within the pages of our journal. We take pride in providing a platform for these emerging researchers to share their novel ideas and findings with the broader scientific community.

In today's rapidly evolving scientific landscape, it is increasingly evident that the challenges we face require a collaborative and interdisciplinary approach. The most complex problems demand a diverse set of perspectives and expertise. Integrative Omics and Applied Biotechnology (IIOAB) Journal has consistently promoted and celebrated this multidisciplinary ethos. We believe that by crossing traditional disciplinary boundaries, we can unlock new avenues for discovery, innovation, and progress. This philosophy has been at the heart of our journal's mission, and we remain dedicated to publishing research that exemplifies the power of interdisciplinary collaboration.

Our journal continues to serve as a hub for knowledge exchange, providing a platform for researchers from various fields to come together and share their insights, experiences, and research outcomes. The collaborative spirit within our community is truly inspiring, and I am immensely proud of the role that IIOAB journal plays in fostering such partnerships.

As we move forward, I encourage each and every one of you to continue supporting our mission. Whether you are a seasoned researcher, a young scientist embarking on your career, or a reader with a thirst for knowledge, your involvement in our journal is invaluable. By working together and embracing interdisciplinary perspectives, we can address the most pressing challenges facing humanity, from climate change and public health to technological advancements and social issues.

I would like to extend my gratitude to our authors, reviewers, editorial board members, and readers for their unwavering support. Your dedication is what makes IIOAB Journal the thriving scientific community it is today. Together, we will continue to explore the frontiers of knowledge and pioneer new approaches to solving the world's most complex problems.

Thank you for being a part of our journey, and for your commitment to advancing science through the pages of IIOAB Journal.

Yours sincerely,

Vasco Azevedo

Vasco Azevedo, Editor-in-Chief
Integrative Omics and Applied Biotechnology
(IIOAB) Journal

ARTICLE

BRAIN TUMOR DETECTION AND CLASSIFICATION MODEL USING OPTIMAL KAPUR'S THRESHOLDING BASED SEGMENTATION WITH DEEP NEURAL NETWORKS

Bakthavachalam Devanathan*, Kaliyappan Venkatachalapathy

Department of Computer and Information Science, Annamalai University, Chidambaram, TN, INDIA

ISSN 0976-3104

ABSTRACT

Brain Tumor (BT) detection and classification is a crucial process for radiologists and the detection of BT at the earlier stage can leads to high survival rate. Therefore, an automated BT detection and classification model is needed to detect the tumor regions at a faster rate. This paper presents a novel brain tumor detection and classification model using an Optimal Kapur's Thresholding based Segmentation with Deep Neural Network, abbreviated as OS-DNN model. The proposed OS-DNN model operates on five major stage, namely preprocessing, segmentation, feature extraction, feature reduction, and classification. Initially, preprocessing of MRI brain images takes place in three ways namely bilateral filtering (BF) based noise removal, contrast limited adaptive histogram equalization (CLAHE) based contrast enhancement and skull stripping. Then, optimal kapur's thresholding based segmentation process takes place and grey wolf optimization (GWO) algorithm is used to optimize the threshold value. Next to that, Discrete Wavelet Transforms (DWT) is applied as a feature extraction technique and kernel principle component analysis (KPCA) is employed as a feature reduction. Finally, DNN model is applied to classify the MRI brain images into normal and abnormal MRI images. The experimentation of the OS-DNN model is carried out using a benchmark Kaggle dataset and the results are examined under different aspects. The simulation outcome ensured that the OS-DNN model is superior to other models with the maximum sensitivity of 97.94%, specificity of 98.08% and accuracy of 98.02%.

KEY WORDS
Brain Tumor, Classification, Deep learning, Feature Extraction, Segmentation

INTRODUCTION

Unlike other tumors, detection of brain tumor using invasive method is very difficult. Therefore, image based diagnosis and classification using Magnetic resonance imaging (MRI) scans is generally practiced. However, computer-aided methods for improved diagnosis and classification of MRI scans are of demand that include better accuracy in tumor detection, segmentation, and classification [1]. Image processing technologies are frequently applied for the purpose of tumor prediction. The key objective of image segmentation is to divide a picture into homogeneous blocks and identifies the structure of every region. Magnetic resonance imaging (MRI) and Computed tomography (CT) scans were employed for examining the presence of BT. MRI scan is highly productive when compared with CT scan and it is not constrained with radiation power [2]. Tumor might be developed with various tissues, single MRI is inadequate to provide to complete information of abnormal tissues. By integrating unique complementary data could extend tumor region which are segmented. A feature of MRI has been applied for segmentation with weighted 3 pictures for all slice's axial. The segmentation principles are highly beneficial mostly at the time of measuring affected tissues. Segmentation is measured as vital procedure while computing MRI which enhances the model's performance. Segmentation contains image partitions that have similar parameters like color, brightness, texture and intensity [3]. Human segmentation of images is assumed to be tedious and time-utilizing operation. Hence, automated segmentation models are needed to develop for effective diagnosis of brain tumor.

Received: 2 June 2020
Accepted: 10 July 2020
Published: 14 July 2020

The combination of Artificial Bee Colony (ABC) and Genetic Algorithm (GA) methodologies finds useful to predict the threshold values. Additionally, statistical features are utilized with support vector machine (SVM) approach as a classifier [4]. El-Dahshan and colleagues have developed feedback pulse coupling network (FPCNN) for image segmentation of BT diagnosis. The DWT, PCA and artificial neural network (ANN) were employed for feature extraction, FS and classification, correspondingly [5]. Similarly, a novel kernel clustering method for MR images segmentation was also developed [6]. These methods have replaced the previous isotropic Gaussian kernel using anisotropic kernel equated by Mahalanobis distance. As fuzzy C-means (FCM) segmentation is applied for detecting affected area in brain MRI. Statistical features as well as SVM are mainly used to process the feature extraction and classification.

Ali et al (2014) defined a new MR image segmentation that depends upon the morphological pyramid with FCM clustering. Initially, wavelet multi-resolution is applied for retaining the spatial context among pixels. Morphological pyramid is utilized to combine final multi-resolution images with actual image which tends to improvise the sharpness and reduce the noise in computed image. Consequently, FCM is used to divide the processed images [7]. Ahmadvand and Kabiri implied a novel segmentation approach according to the Markov random field as well as feature vector for the combination of spatial and spectral data for MRI image segmentation [8]. In 2017, Cabria and Gondra provided a segmentation technique named as Potential Field Segmentation (PFS) [9]. It is evident that, the developed method is capable of classifying MR images effectively. Also, the MRI segmentation techniques are viewed as successful image segmentation schemes which are applied in this literature.

***Corresponding Author**
Email:
devacisau@gmail.com

IIOAB JOURNAL
ISSN: 0976-3104

Cigaroudy and Aghazadeh applied a new multiphase segmentation technique which depends on the combination of intensity function, eigenvector of Hessian matrix and Curvelet [10]. Similarly, Akbarizadeh developed a new model named as Synthetic Aperture Radar (SAR) for image segmentation which depends upon the simple segmentation processes. The presented method compounds the intensity data and input image texture with the help of Cellular Learning Automata (CLA) for segmenting SAR images [11]. Rahmani and Akbarizadeh developed an unsupervised feature learning approach according to the unification of spectral clustering and sparse coding SAR image segmentation [12]. Spectral clustering is defined as an image segmentation model which makes feasible combination of features and cues. Sparse coding is referred as an unsupervised learning that identifies the patterns of high-level data semantics. Furthermore, it provides alternate collaboration of texture and color features for the segmentation of polarimetric SAR (PolSAR) image. Though various segmentation techniques are available, still there is a need to develop automated segmentation and classification models for BT diagnosis for achieving maximum classification performance.

This paper introduces novel BT detection and classification model using an Optimal Kapr's Thresholding based Segmentation and DNN model, abbreviated as OS-DNN model. The proposed OS-DNN model initially undergoes preprocessing to improve the classification performance by noise removal, contrast enhancement, and skull stripping. Then, optimal Kapur's thresholding based segmentation process takes place and grey wolf optimization (GWO) algorithm is used to optimize the threshold value. Then, discrete wavelet transform (DWT) based feature extraction and kernel principal component analysis (KPCA) based feature reduction process takes place. At last, deep neural network (DNN) model is applied to classify the MRI brain images into normal and abnormal MRI images. The experimentation of the OS-DNN model is carried out using a benchmark Kaggle dataset and the results are examined under different aspects.

METHODS

The overall working procedure involved in OS-DNN method is illustrated in Fig. 1. As depicted, the projected OS-DNN model undergoes pre-processing, GWO-KT based segmentation, DWT relied feature extraction, KPCA based feature reduction, and classification using DNN model. These processes are explained in the following sections.

Preprocessing: Initially, the input image undergoes preprocessing in three stages namely bilateral filtering (BF) based noise removal, contrast limited adaptive histogram equalization (CLAHE) based contrast enhancement, and skull stripping.

GWO-KT based Segmentation: In early decades, Kapur's image segmentation was mainly applied for segmenting gray scale images with the help of histogram's entropy. It identifies an optimal T value that enhances the entire entropy [13]. Suppose $\mathbf{T} = [t_1, t_2, \ldots, t_{k-1}]$ be a vector of image threshold. Next, Kapur's entropy would be represented as

$$I_{max} = f_{kapur}(T) = \sum_{j=1}^{k} H_j^C \; for C\{1,2,3\} \qquad (1)$$

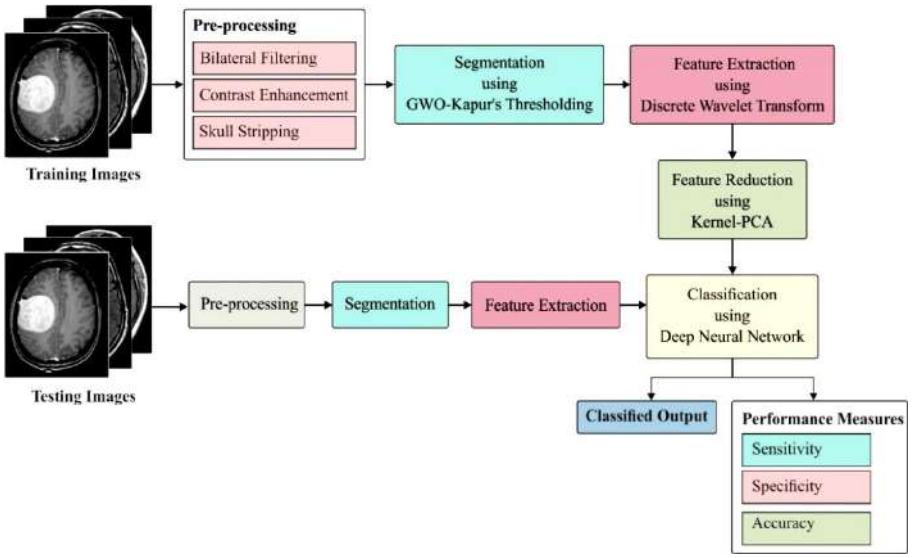

Fig. 1: Working Principle of OS-DNN Model

Basically, entropy is determined in an independent manner according to the t value. The multi-level thresholding issue can be demonstrated as,

$$H_1^C = \sum_{j=1}^{t_1} \frac{Ph_j^C}{\omega_0^C} \ln\left(\frac{Ph_j^C}{\omega_0^C}\right)$$
$$H_2^C = \sum_{j=t_{1+1}}^{t_2} \frac{Ph_j^C}{\omega_1^C} \ln\left(\frac{Ph_j^C}{\omega_1^C}\right) \quad (2)$$
$$\vdots$$
$$H_k^C \sum_{j=t_{k+1}}^{L} \frac{Ph_j^C}{\omega_{k-1}^C} \ln\left(\frac{Ph_j^C}{\omega_{K-1}^C}\right)$$

where Ph_j^C denotes the probability distribution and $\omega_0^C, \omega_1^C, \omega_{k-1}^C$ denotes the probability action for K levels. At the time of multi-level thresholding process, it is needed to decide the optimum threshold value T that maximize the objective function $f(T)$. Here, the maximization of ($f(T)$) is done by the use of GWO algorithm.

GWO method is deployed by [14], which has been evolved from the hunting nature of grey wolves. These wolves are assumed to be top-level predators and reside in a group of 5-12 wolves. Based on the hunting nature, the wolves are categorized into alpha (α), beta (β), delta (δ), and omega. Initially, dominant wolves are named to be original dominators for the team, as it is capable of making decisions according to the residing location, hunting, and so on. It is termed as dominant wolves. Additional wolves follow the rules of alpha wolves. The next level wolves are beta that makes decisions in absence of alpha wolves. It is given with some rights of finding solutions for alpha wolves and offers a response accordingly. Thirdly, the delta wolves are the consecutive level wolves, called as subordinate wolves. It comes under the type of elders, sentinels, hunters, scouts, and caretakers. The delta wolves monitor the task of alpha and beta wolves and manage the subsequent levels known as omega wolves. At last, omega is final ranking wolves and treated as scapegoat. It applies the process recommended by alpha wolves. The omegas are ineffective wolves, and it help is resolving the internal problems.

Hunting process of wolves are categorized into tracking and chasing, pursuing and surrounding until it terminates moving, and attacking the prey. GWO is operated using exploration and exploitation phase. The exploitation phase performs the task of exploring best solutions in local search space. The grey wolves surround and attack the prey at the time of searching better solutions from local search space. When the prey is surrounded, the wolves identify prey's location and attack them. In this approach, the position vectors of a prey have been implied and find the agents that change the location according to accomplished optimal solution which is illustrated as:

$$\vec{D} = \left|\vec{C}.\overrightarrow{Q_p}(n) - \vec{Q}(n)\right| \quad (3)$$

$$\vec{Q}(n+1) = \overrightarrow{Q_p}(n) - \vec{A}.\vec{D} \quad (4)$$

Where n is the recent iteration, $\vec{A}$ and $\vec{C}$ are coefficient vectors, position vector of a prey as $\overrightarrow{Q_p}(n)$, $\vec{Q}$ denotes the position vector, || implies absolute value and . shows an element by element improvement. The vectors $\vec{A}$ and $\vec{C}$ are expressed as:

$$\vec{A} = 2\vec{a}.\vec{r} - \vec{a} \quad (5)$$

$$\vec{C} = 2.\vec{r} \quad (6)$$

In hunting phase, grey wolves are triggered by α and only the contributions are provided to β and δ. Initially, the optimum solution cannot be found as it consumes maximum amount of energy in hunting phase, α is the primary better candidate solution, beta defines upcoming optimal candidate solution and lastly delta represents consequent better candidate solution. The 3 solutions are reached and extended to change the position of lower ranking solution which demonstrates the hunting phase:

$$\begin{aligned}\vec{D}_\alpha &= |\vec{C}_1 * \vec{Q}_\alpha - \vec{Q}\ | \\ \vec{D}_\beta &= |\vec{C}_2 * \vec{Q}_\beta - \vec{Q}\ | \\ \vec{D}_\delta &= |\vec{C}_1 * \vec{Q}_\delta - \vec{Q}\ |\end{aligned} \quad (7)$$

Where $\vec{D}_\alpha$, $\vec{D}_\beta$, and $\vec{D}_\delta$ are changed distance vector among the α, β and γ positions to alternate wolves and $\vec{C}_1$,$\vec{C}_2$, and $\vec{C}_3$ are 3 coefficient vector applied in varying distance vector. $\vec{Q}$ refers the position of vector of grey wolf (omega).

$$\begin{aligned}\vec{Q}_1 &= \vec{Q}_\alpha - \vec{A}_1 * \vec{D}_\alpha \\ \vec{Q}_2 &= \vec{Q}_\beta - \vec{A}_2 * \vec{D}_\beta \\ \vec{Q}_3 &= \vec{Q}_\delta - \vec{A}_3 * \vec{D}_\delta\end{aligned} \quad (8)$$

IIOAB JOURNAL
ISSN: 0976-3104

where $\vec{Q}_1$ is novel position vector by exploiting the α position $\vec{Q}_\alpha$ and distance vector $\vec{D}_\alpha$, $\vec{Q}_2$ means a novel position vector is accomplished under the application of β position $\vec{Q}_\beta$ and distance vector $\vec{D}_\beta$, $\vec{Q}_3$ shows the novel position vector determined by applying delta position $\vec{Q}_\delta$ as well as distance vector $\vec{D}_\delta$, and $\vec{A}_1$, $\vec{A}_2$, and $\vec{A}_3$ are 3 coefficient vectors are evaluated.

$$\vec{Q}(n+1) = \frac{\sum_{i=1}^{k} \vec{Q}_i}{n} \quad (9)$$

where $\vec{Q}(n+1)$ signifies new position vector is estimated by using α, β and δ (k=3).

DWT based Feature extraction: In general, DWT is an efficient deployment of WT with the help of dynamic scales as well as positions. A basic DWT is established in [15]. Assume that $u(t)$ refers square-integrable function, and continuous WT of $u(t)$ related to provided wavelet $\psi(t)$ is expressed as

$$W_\psi(a,b) = \int_{-\infty}^{\infty} u(t)\psi_{a,b}(t)dt \quad (10)$$

Where

$$\psi_{a,b}(t) = \frac{1}{\sqrt{a}}\psi\left(\frac{t-a}{b}\right) \quad (11)$$

In this approach, the wavelet $\psi_{ab}(t)$ is acquired from native wavelet $\psi(t)$ using translation and dilation, where$a$ implies a dilation factor and$b$ denotes translation parameter. The Harr wavelet is a significant wavelet, which is simple and mostly employed in many domains.

Eq. (11) is discretized by retaining a and $b$for discrete lattice $(a = 2^p \& a > 0)$ to provide DWT as described below:

$$\mathrm{ca}_{j,k}(n) = \mathrm{DS}\left[\sum_n u(n) g_j^*(n - 2^j k)\right]$$
$$\mathrm{cd}_{j,k}(n) = \mathrm{DS}\left[\sum_n u(n) h_j^*(n - 2^j k)\right] \quad (12)$$

Here $\mathrm{ca}_{j,k}$ and $\mathrm{cd}_{j,k}$ means the coefficients of approximation components and detail components, correspondingly; $g(n)$ and $h(n)$ are low-pass filter and high-pass filter; j and k shows the wavelet scale as well as translation factors, and DS is the down sampling.

In case of 2D images, the DWT is used for all dimensions. It is composed with 4 sub-bands such as LL, LH, HH, and HL images at every scale. The sub-band LL is applied for consecutive 2D DWT. The LL sub-band is named as approximation unit of an image, while LH, HL, and HH sub-bands are known to be expanded image components. The decomposition level has been enhanced, and then coarser approximation component can be reached. Therefore, wavelets provide easy hierarchical approach to interpret the image details.

Feature Reduction using KPCA: The existence of massive features leads to maximum processing time and requires more storage. Besides, it makes the classification process difficult, known as curse of dimensionality and is needed to minimize the feature count. KPCA is an extended version of PCA, which has been evolved by kernel models. Under the application of a kernel, the actual linear task of PCA was processed in regenerating kernel Hilbert space. The component of PCA can be established for clustering, and it is monitored that, if N points could not be a general term, then it is linearly classified in $d < N$ dimensions, it is prominently separated in a linear manner in $d \geq N$ dimensions. The given N points x_i, when it is mapped into N-dimensional space with

$$\Phi(u_i) where \Phi: \mathbb{R}^d \rightarrow \mathbb{R}^N, \quad (13)$$

It is simply manufactured as a hyper-plane which classifies the points into random clusters. Obviously, Φ develops the autonomous vectors randomly, thus no covariance in eigen decomposition could be explicitly processed in linear PCA.

DNN based Classification: Once the feature reduction process is done, classification process takes place on the feature values or vectors. Normally, classification is represented as a boundary among the classes for labeling the classes depending upon the determined features. Here, DNN is applied as a classification model. The DNN generally operated on FFNN and is defined as an unsupervised pre-training model which uses greedy layer wise training. In this approach, the data flow from input layer to output layer with no looping function. The benefit in DNN classification is the nature of classifying the feasibilities of missing values is minimum. It shows a single layer in unsupervised pre-training level [16]. The DNN

IIOAB JOURNAL
ISSN: 0976-3104

assigns a classification score $t(x)$ over a prediction time. Each input data sample $x = [x_1, \cdots\cdots x_N]$ is a forward pass. Then, f signifies the function where a series of layers for processing, that is implied in Eq. (14)

$$Z_{ij} = X_i W_{ij}; Z_j = \sum_i Z_{ij} + b_j; X_j = g(Z_j), \qquad (14)$$

where input layer is depicted as x_i, output layer is x_j, and w_{ij} are modelling parameters and $g(Z_i)$ analyze the pooling function. Layer-wise relevance propagation degrades the classification result $f(x)$ with respect to relevance's r_i with input component x_i, and applied on classification process as defined in Eq. (15):

$$f(x) = \sum_i r_i \qquad (15)$$

where $r_j > 0$ is the positive evidence that supports the classification decision and $r_j < 0$ shows the negative evidence of classification; else, it named as neutral evidence, even though related attribute r_i is evaluated using Eq. (16).

$$r_i = \sum_j \frac{zij}{\Sigma_i zij}. \qquad (16)$$

The typical structure of DNN is shown in Fig. 2. The DNN is capable to analyze the unwanted feature correlation of input. It offers a hierarchical feature learning technology. Hence, higher-level features can be accomplished from minimum level features using greedy layer wise unsupervised pre-training data. Therefore, the main aim of DNN is to resolve the tedious functions and results in high-level abstraction.

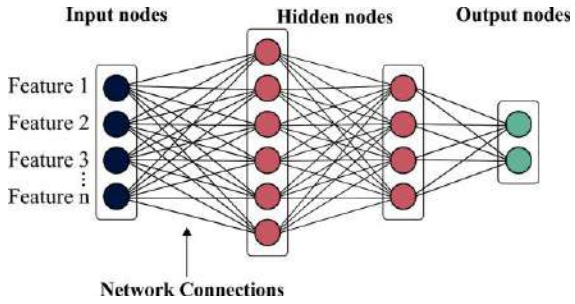

Fig. 2: Architecture of Deep Neural Networks (DNN)

RESULTS AND DISCUSSION

Dataset used: The working function of projected approach is verified with the application of standard dataset from Kaggle [17]. The dataset comprises a total of 98 normal MRI brain images and 155 abnormal MRI brain images. The size of the images varies between 192*192 and 630*630.

Results Analysis: A sample visualization of the results offered by the presented OS-DNN model on the applied images is illustrated in Fig. 3. The original test images are shown in Fig. 3a, contrast enhanced image is depicted in Fig. 3b, skull stripped image is provided in Fig. 3c, segmented image in Fig. 3d, and finally, classified image in Fig. 3e. The figures clearly ensured that the OS-DNN model has effectively classified the images into its appropriate class labels.

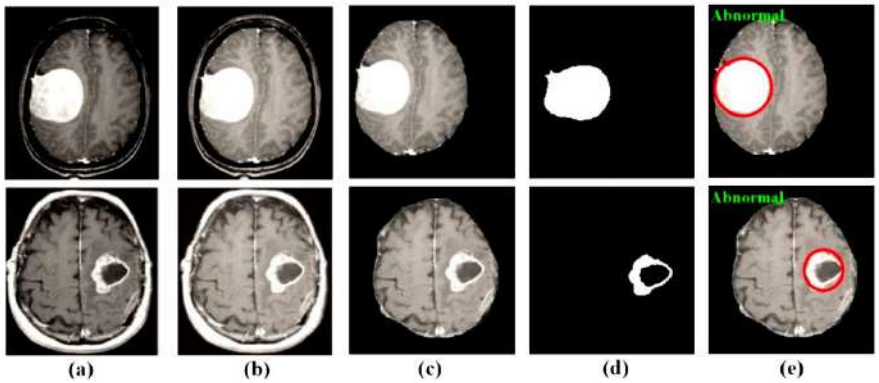

Fig. 3: a) Original b) Contrast Enhanced c) Skull stripped d) Segmented e) Classified

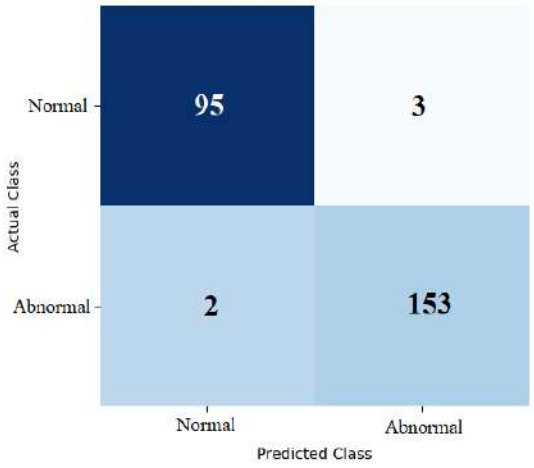

Fig. 4: Confusion Matrix of OS-DNN

[Fig. 4] displays the confusion matrix of the OS-DNN model generated at the time of execution time. The figure clearly stated that the proposed OS-DNN model has properly classified a set of 95 images as normal out of 98 and 153 images as abnormal out of 155. These values provided that the OS-DNN model has effectively classified the MRI brain images.

A detailed comparative study of the results offered by the OS-DNN and existing models is shown in Table 1.

Table 1: Result Analysis of Existing with Proposed Method in term of Sensitivity, Specificity, Accuracy

Methods	Sensitivity	Specificity	Accuracy
Proposed OS-DNN	97.94	98.08	98.02
SVM (kernel polynomial)	94.73	97.59	96.18
SVM (kernel RBF)	95.62	83.71	89.88
Decision tree	97.88	91.71	94.95
CART	88.00	80.00	84.00
Random Forest	96.00	80.00	88.00
k-NN	80.00	80.00	80.00
Linear SVM	96.00	80.00	88.00
Anitha et al. [18]	91.20	93.40	93.30
Urban et al. [19]	92.60	93.00	93.30
Pereira et al. [20]	94.20	94.40	94.60
Islam et al. [21]	94.30	95.10	95.90
Selvapandian et al. [22]	96.20	95.10	96.40

Fig. 5 depicts the classification result analysis of OS-DNN with related models with respect to accuracy. The figure refers that the k-NN model has demonstrated poor classifier results with the accuracy of 80%. Besides, the CART approach has showcased considerable accuracy of 84%. On the other hand, the RF as well as Linear SVM models have shown better and identical accuracy values of 88%. Additionally, the SVM has displayed considerable accuracy of 89.88%. Simultaneously, the approaches used by Anitha et al. (2017) [18] and Urban et al. (2014) [19] have exhibited even more and identical accuracy values of 93.30%. Additionally, the model deployed by Pereira et al. (2016) [20] and DT models attempted to indicate applicable results with the accuracy of 94.60% and 94.95% correspondingly. In addition, the method deployed by Islam et al. (2013) [21] has accomplished an accuracy of 95.90%. Moreover, the SVM (kernel polynomial) technique has showcased better accuracy of 96.18%. In line with this, the Selvapandian et al. (2018) [22] framework has exhibited near optimal results with the accuracy of 96.40%. At last, the OS-DNN model has showcased optimal outcome than related models with the higher accuracy value of 98.02%.

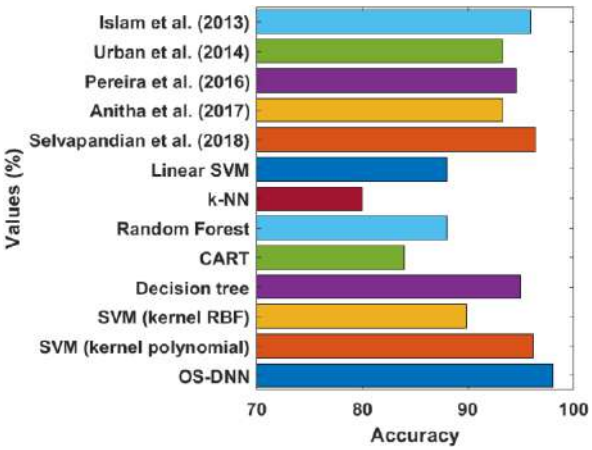

Fig. 5: Accuracy analysis of OS-DNN with other models

From the Table-1 and Fig-5, it is obvious that the OS-DNN model can be applied as an effective diagnosis and classification model for BT from MRI brain images.

CONCLUSION

Effective detection and classification of BT has received maximum attention among research community and medical institutions. This paper has presented novel BT detection and classification model using OS-DNN model. The proposed OS-DNN model initially undergoes preprocessing to improve the classification performance by noise removal, contrast enhancement, and skull stripping. Followed by, GWO-KT based segmentation, DWT based feature extraction, KPCA based feature reduction, and DNN based classification processes are carried out. The proposed OS-DNN model effectively detects and classifies the affected regions in the MRI image. The experimentation of the OS-DNN model is carried out using a benchmark Kaggle dataset and simulation outcome ensured that the OS-DNN model is superior to other models with the maximum sensitivity of 97.94%, specificity of 98.08% and accuracy of 98.02%. In future, the performance of the OS-DNN model can be improved by the use of hyper parameter tuning models to effectively choose the parameters involved in DNN.

CONFLICT OF INTEREST
There is no conflict of interest.

ACKNOWLEDGEMENTS
None

FINANCIAL DISCLOSURE
None

REFERENCES

[1] Abd-Ellah MK, Awad AI, Khalaf AAM, Hamed HFA. [2019] A review on brain tumor diagnosis from MRI images: Practical implications, key achievements, and lessons learned. Magn Reson Imaging, 61:300-318.

[2] Patel J, Doshi K. [2014] A study of segmentation methods for detection of tumor in brain MRI. Advance in Electronic and Electric Engineering, 4(3):279-84.

[3] Logeswari T, Karnan M. [2010] An improved implementation of brain tumor detection using segmentation based on hierarchical self-organizing map. International Journal of Computer Theory and Engineering, 2(4):591.

[4] Beno MM, Rajakumar BR. [2014] Threshold prediction for segmenting tumour from brain MRI scans. International journal of imaging systems and technology, 24(2):129-37.

[5] El-Dahshan ES, Mohsen HM, Revett K, Salem AB. [2014] Computer-aided diagnosis of human brain tumor through MRI: A survey and a new algorithm. Expert systems with Applications, 41(11):5526-45.

[6] Liao L, Zhang Y. [2011] MRI image segmentation based on fast kernel clustering analysis. Frontiers of Electrical and Electronic Engineering in China, 6(2):363-73.

[7] Ali H, Elmogy M, El-Daydamony E, Atwan A. [2015] Multi-resolution mri brain image segmentation based on morphological pyramid and fuzzy c-mean clustering. Arabian Journal for Science and Engineering, 40(11):3173-85.

[8] Ahmadvand A, Kabiri P. [2016] Multispectral MRI image segmentation using Markov random field model. Signal, Image and Video Processing, 10(2):251-258.

[9] Cabria I, Gondra I. [2017] MRI segmentation fusion for brain tumor detection. Information Fusion, 36:1-9.

[10] Cigaroudy LS, Aghazadeh N. [2017] A multiphase segmentation method based on binary segmentation method for Gaussian noisy image. Signal, Image and Video Processing, 11(5):825-8231.

[11] Akbarizadeh G. [2013] Segmentation of SAR satellite images using cellular learning automata and adaptive chains. J. Remote Sens. Technol, 1(2):44-51.

[12] Rahmani M, Akbarizadeh G. [2015] Unsupervised feature learning based on sparse coding and spectral clustering for segmentation of synthetic aperture radar images. IET Computer Vision, 9(5):629-638.

[13] Rajinikanth V, Satapathy SC, Fernandes SL, Nachiappan S. [2017] Entropy based segmentation of tumor from

brain MR images–a study with teaching learning based optimization. Pattern Recognition Letters, 94:87-95.
[14] Mirjalili S, Mirjalili SM, Lewis A. [2014] Grey wolf optimizer. Advances in engineering software, 69:46-61.
[15] Zhang Y, Wang S, Ji G, Dong Z. [2013] An MR brain images classifier system via particle swarm optimization and kernel support vector machine. The Scientific World Journal, DOI: 10.1155/2013/130134.
[16] Suresh R, Rao AN, Reddy BE. [2019] Detection and classification of normal and abnormal patterns in mammograms using deep neural network. Concurrency and Computation: Practice and Experience, 31(14):5293.
[17] https://www.kaggle.com/navoneel/brain-mri-images-for-brain-tumor-detection
[18] Anitha R, Raja DSS. [2017] Segmentation of glioma tumors using convolutional neural networks. International Journal of Imaging Systems and Technology, 27(4):354-360.
[19] Urban G, Bendszus M, Hamprecht FA, Kleesiek J. [2014] Multimodal brain tumor segmentation using deep convolutional neural networks. MICCAI Brain Tumor Segmentation (BraTS) Challenge. Proceedings, 31– 35, Boston, MA, USA.
[20] Pereira S, Pinto A, Alves V, Silva CA. [2016] Brain Tumor Segmentation Using Convolutional Neural Networks in MRI Images. IEEE Transactions on Medical Imaging, 35: 1240- 1251.
[21] Islam A, Reza S, Iftekharuddin KM. [2013] Multifractal texture estimation for detection and segmentation of brain tumors. IEEE Trans. Biomed. Eng., 60:3204–3215.
[22] Selvapandian A, Manivannan K. [2018] Fusion based glioma brain tumor detection and segmentation using ANFIS classification. Computer methods and programs in biomedicine, 166: 33-38.

IIOAB JOURNAL

ARTICLE

COMBUSITON AND EMISSION ANALYSIS OF OXYGENATED MUSTARD OIL BIODIESEL WITH EXHAUST GAS RECIRCULATION IN COMPRESSION IGNITION ENGINE

Elavarasan Govindaraj*, Sethuraman Narayanan, Karthikeyan Duraisamy

Dept. of Mechanical Engineering, Faculty of Engineering & Technology, Annamalai University, Chidambaram, TN, INDIA

ISSN 0976-3104

ABSTRACT

Diesel Engines are more suitable for using Biodiesel fuel extracted from oil plants. In this research, biodiesel was separated from the mustard oil and it was blended with the diesel in the ratio of 5%, 10%, 15%, and 20%. All the blends were added with 10% of Di-tetra-butyl-peroxide and it was tested in a diesel engine to study its performance and emission characteristics. The 20% of mustard oil mix was included with the 15% of Exhaust Gas Recirculation to lessen NOX discharges and its exhibition and emanation characters were contrasted and that of others. From the results, the CO emissions reduced by 9.5% and HC by 2.4% the NOX emissions were decreased by 4.7% for the 20% blend of mustard oil with 15% EGR when compared to diesel fuel.

KEY WORDS
Biodiesel, Brake thermal efficiency, Mustard oil, DTBP additive, NOX emission reduction

Received: 16 June 2020
Accepted: 24 July 2020
Published: 28 July 2020

***Corresponding Author**
Email:
elavarasanmit@gmail.com

INTRODUCTION

Infection The automobile sector is the major consumer of petroleum-based products and it is responsible for the release of various harmful emissions into the environment like HC, CO, NOX, soot and greenhouse gases like CO_2 [1]. To control the release of these harmful exhaust gases into the environment various countries have initiated and implemented different pollution standards to the Automobile manufacturers according to the vehicle type in order to keep the air quality clean. As the crude oil reserves in our country are less than 0.5% of world total reserves, it is important to locate an elective wellspring of fuel for powering internal combustion engines [2]. It is likewise seen that the raw petroleum-based engines release harmful emissions and this will pollute the environment. It is necessary to move towards an alternative source of fuel to reduce our dependence upon the petroleum-based products and also to satisfy the rigorous emission norms. In recent times, EURO VI emission norms are recommended for the automobiles. As there is no major modification required for using alternative fuel, diesel engines are preferred to use the alternative fuel. Oil extracted from vegetable oils is becoming trending in the field of alternative fuels to investigate its performance and emission characters [3]. The oil extracted from the vegetable seeds has more triglycerides and this is suitable for blending it with diesel fuel. The glycerol content in the vegetable oil can be evacuated by the trans-esterification process, before mixing it with the diesel. As a result of the more oxygen content in the biodiesel, the creation of hydrocarbon (HC) and carbon monoxide (CO) is extremely less [4]. Based on the environment and the availability of the oilseeds, the biodiesel used can be selected. The yield of mustard oil is 227 to 531 liters per acre, so it was selected for the production of biodiesel through the trans-esterification process [5]. Researches in Di-tetra-butyl-peroxide (DTBP) additive effect on biodiesel proved that it can reduce the HC, CO & NOX emissions simultaneously on biodiesel [6]. Many types of research in the EGR have proved that it can reduce the NOX emission formation for diesel as well as biodiesel in the CI engine [7-9]. In this research, we have examined the combined effect of the DTBP additive as well as the EGR produced by the Mustard oil biodiesel blends on the performance and emission characters. In this research, the mustard oil-based biodiesel was added with Di-tetra-butyl-peroxide (DTBP) and mixed with diesel in different proportions and it was tried in a diesel motor with and without Exhaust Gas Recirculation (EGR).

PREPERATION OF BIODIESEL

The oil separated from the mustard seed experienced a trans-esterification procedure to lessen the fuel viscosity by expelling the free unsaturated fat substance. In this process, initially, the raw oil was mixed with the methanol (ratio of oil to methanol is 5:1) in the presence of a small amount of sodium hydroxide (16-18 grams per lire of raw oil) [10 - 15]. At that point, it was ceaselessly mixed and warmed and kept up at a temperature of 65°C for about an hour and afterward moved into a separation funnel to settle down. After 5-7 hours, the fatty acid (in the form of glycerol) present in the oil was settled at the base of the pipe and the biodiesel on the top. The glycerol was separated and removed, the remaining biodiesel was washed with deionized water for removing extra soap content and the final product is heated again to remove the traces of water particles [16 - 18]. The different properties of diesel and mustard oil were estimated by the ASTM measures and given in [Table 1]. The kinematic viscosity, flash point, fire point cloud point, pour point, the density of the mustard oil biodiesel is more noteworthy than that of the unadulterated diesel fuel which influences the fuel evaporation qualities. The calorific estimation of the mustard oil biodiesel is lesser than that of the diesel which can prompt increment in the fuel utilization. These properties of the fuel impact greatly on the performance as well as the emission characters of the engine.

IIOAB JOURNAL
ISSN: 0976-3104

Table 1: Comparison of properties of mustard oil biodiesel and diesel

S.No	Properties	Mustard oil	Diesel
1	Kinematic Viscosity (mm^2/s)	6.6	4.2
2	Flash point (˚C)	158	57
3	Fire point (˚C)	187	74
4	Cloud point (˚C)	4	-12
5	Pour point (˚C)	-12	-23
6	Specific gravity	0.895	0.841
7	Cetane Number	38	50
8	Calorific value (kJ/kg)	39857	44950

The readied Mustard oil biodiesel was mixed with diesel in the proportion of 5:95, 10:90, 15:85, and 20:80 by volume and assigned as MB5, MB10, MB15 and MB20 separately. Since the cetane number of mustard oil is low, it is difficult to self-ignite the fuel. Hence, 10% of Di-tetra-butyl-peroxide (DTBP) was added to all the blends as cetane improvers to accelerate the ignition process. This also acts as an oxygenated additive to reduce HC, CO simultaneously. Studies have also been made by using octanol and heptanol additives with mustard oil blends and the results are found to be impressive [19-20]. Because of the high thermal stability of DTBP and commercial availability, it was selected as an additive. DTBP enhances the rate of chain initiation for HC oxidation by giving up free radicals through decomposition during the ignition delay period.

METHODS

Biodiesel mixes were tried in a solitary chamber, 4-stroke, diesel engine. The particular of the motor was given in [Table 2]. The heap on the motor was controlled and changed by shifting the heap on the swirl current dynamometer with the assistance of a burden cell unit. The motor speed set at 1500 rpm. The presentation and outflow characteristics were estimated at various brake powers (1.6 kW, 3.2 kW, 4.8 kW, 6.4 kW, and 8 kW) of the motor. The in-chamber pressure was estimated for 100 motorcycles utilizing a weight transducer mounted on the chamber head and recorded in the PC utilizing "AVL Indicom programming". The recorded weight information esteems were arrived at the midpoint of to figure the Heat discharge rate (HRR). Exhaust emanations like Hydrocarbon (HC), Carbon monoxide (CO), and nitrogen oxides (NOX) were estimated from "AVL Digas analyzer". The smoke thickness was estimated utilizing "AVL smoke meter". The time taken for utilization of 10cc of fuel from the burette was noted utilizing stopwatch at all test conditions. The engine experimental layout was shown in [Fig. 1].

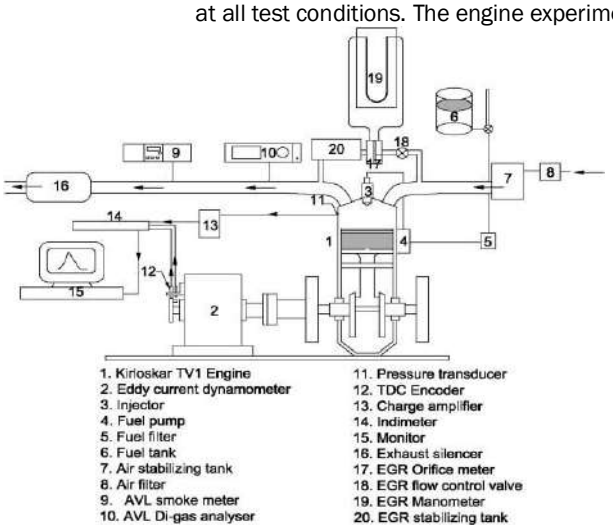

Fig. 1: Engine experimental layout

Table 2: Engine specification

Make	Kirlosar-TV 1
General details	Four stroke, compression ignition, water cooled, direct injection
Bore	87.5 mm
Stroke	110 mm
Compression ratio	17.5:1
Rated speed	1500 rpm
Injection pressure	220 bar
Fuel injection timing	23 BTDC
Rated output	8 kW
Speed	1500 rpm

IIOAB JOURNAL
ISSN: 0976-3104

Initially, the engine was warmed up by running it with diesel fuel for 15 minutes to achieve a stable operating condition. The speed of the engine was maintained constant at 1500rpm at all loads by adjusting the fuel flow rate manually. Then the engine was operated with all the prepared test fuels with a break of 30 minutes between each fuel to cool the engine. A 15% EGR was used with the MB20 blend. The percentage of EGR was controlled by adjusting the flow valve manually with the help of orifice and manometer reading. The exhaust gas analyzer probe was inserted in the exhaust tailpipe. After each measurement, the probe was taken out and exhaust gases were purged from the probe. The exhaust emission was measured three times for each test condition and averaged. The averaged value was considered for the analysis.

RESULTS AND DISCUSSION

The aftereffects of Brake Thermal Efficiency (BTE) of the diesel motor powered by MB biodiesel – diesel mixes appeared in the [Fig. 2]. From [Fig. 2], it was deduced that the BTE of all the test fuels is by all accounts expanded up to 80% (6.4kW) load and indicated a slight drop at 100% (8 kW) load. The BTE was diminished with increment in MB biodiesel mix rate [21]. At full burden, the test fills MB5 and MB20 indicated a 3.5% and 8.5% decrease in BTE separately when contrasted with slick diesel. This is on the grounds that the vitality thickness of mustard oil biodiesel was not as much as diesel. A similar impact likewise expanded the particular fuel utilization for MB biodiesel mixes [21]. The EGR further decreased the BTE of MB20 by 2.7% compared to without EGR. This is due to the deterioration of in-cylinder combustion caused by the dilution of intake air by exhaust gases. The EGR reduced oxygen concentrations in the intake and also cause a drop in combustion temperature which in turn affects the combustion efficiency.

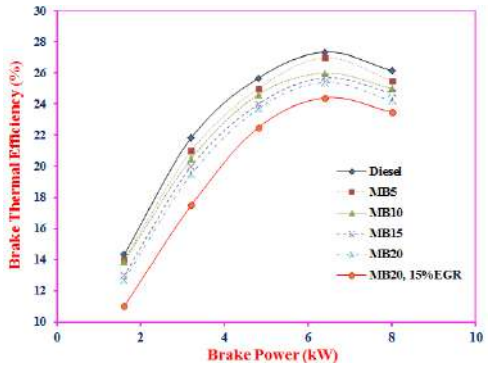

Fig. 2: BTE (%) vs. Brake Power (kW)

The [Fig. 3] shows that the smoke emanation is decreased with increment in the biodiesel mix. Typically the smoke discharge will increment with increment in the biodiesel mix as more measure of fuel is gathered in the burning chamber because of lower Cetane number of biodiesel [24-26]. The unadulterated diesel fuel shows the most extreme smoke discharge while MB20 shows the least smoke outflow among the test powers. At full burden condition, the MB20 shows a smoke decrease of 44.5% than that of diesel, this is a direct result of the impact of innate oxygen present in the mustard oil biodiesel ester and furthermore in the additional DTBP added substance which advanced more oxidation of sediment molecule. The MB20 with EGR shows higher smoke than without EGR but still exhibits a smoke reduction of 11.4% when compared to diesel. The reason for the increase in smoke with EGR for MB20 is due to a reduction in combustion temperature which favors condensation of Poly Aromatic Hydrocarbon (PAH) and polymerization of lower-order molecules to form a large unsaturated molecule. These two destined to form soot and thereby increasing the smoke.

[Fig. 4] demonstrates that the CO emanation for the MB20 is seen to be least among the test energizes because of the accessibility of oxygen in its sub-atomic structure which elevated CO oxidation to CO2. As the Brake mean effective pressure expands, the arrangement of the CO discharges will increment [27]. Indeed, even the brake mean effective pressure is more in the MB fuel contrasted with that of the diesel; the development of the CO emanation is not as much as that of the diesel [28]. The discharge arrangement of the CO outflow is diminished with the expansion in the mix, the most extreme decrease of 28.5% than diesel was seen when MB20 was tried at 8 kW brake power. This is because of the nearness of oxygen atom in the mustard oil biodiesel and DTBP added substance which advances CO oxidation. The MB20 with 15% EGR shows the CO formation of 6.38% lesser than that of the diesel.

From the [Fig. 5], it is seen that the NOX discharges expanded with increment in the biodiesel mix rate in light of the advancement of high brake mean effective pressure in the ignition chamber that can bring about high burning temperature and furthermore because of the essence of oxygen in the sub-atomic structure of MB and DTBP that upgraded the fuel oxidation and improved the ignition [30]. It is obviously observed from [Fig. 5] that the arrangement of NOX emanation is more in MBD20 without EGR, on account of the higher in-chamber pressure created from the MB fuel [29] which is brought about by high pinnacle heat discharge rate. High ignition temperature and oxygen are the hotspots for the development of NOX. Thus, the NOX discharge is expanded with increment in the mix rate. The NOX emission is increased by 1.5%, 4.7%, 7.9%, and 11.1% for the MB5, MB10, MB15, and MB20 respectively, but a reduction of 4.7% is observed with

15% EGR when compared to that of diesel. The MB20 with 15% EGR has shown lesser because of the dilution effect which reduced both combustion temperature and oxygen concentration.

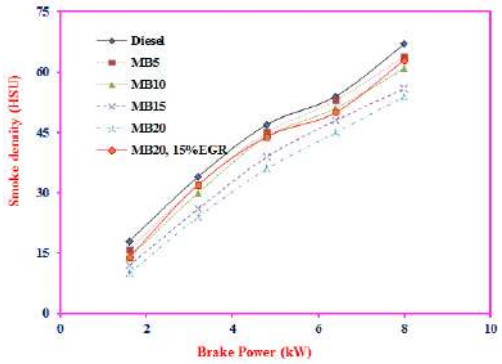

Fig. 3: Smoke (HSU) vs. Brake Power (kW)

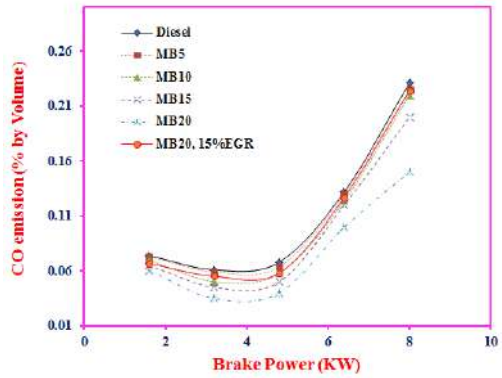

Fig. 4: Brake Power vs. CO emission

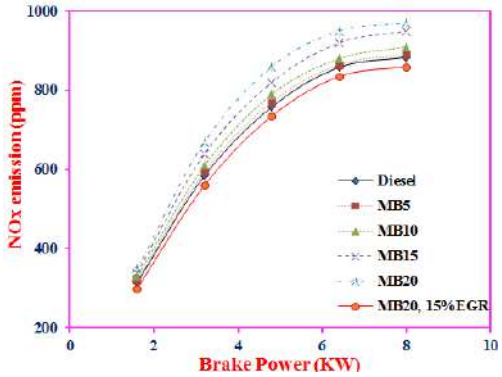

Fig. 5: Brake Power vs. NOX emission.

[Fig. 6] shows the HC outflow, all things considered, HC emanations are created in the motor because of the blend of air-fuel blend fixation, poor dissipation and blending attributes of fuel and temperature [31]. The HC discharge is diminished by about 4.7%, 7.1%, 11.9%, and 16.6% than that of diesel for MB5, MB10, MB15, and MB20 individually. Indeed, even with the expansion of 15% EGR, MB20 indicated a decrease of 2.4% HC emanation than that of diesel. Since biodiesel mixes improved the oxidation of hydrocarbon through the inborn oxygen particle in it. Diesel fuel has demonstrated the greatest HC outflow among the test energizes. This might be expected to in-complete ignition. The DTPB added substance likewise impacted HC discharges by improving hydrocarbon oxidation by expanding the oxygen focus in the biodiesel mixes. The EGR restrict the complete combustion by reducing the temperature which affects the evaporation of fuel droplets inside the combustion chamber and oxygen content in the intake air.

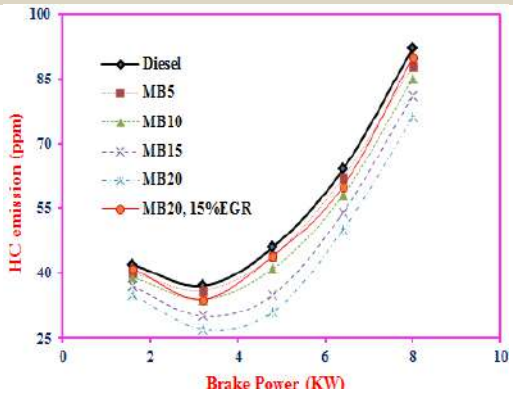

Fig. 6: HC emission vs. Brake Power

[Fig. 7] demonstrates that the greatest chamber pressure was accomplished for the MB20 fuel, this is a direct result of consuming of higher thickness bead of biodiesel mixes that is brought about by high thickness and consistency nature of biodiesel. This impact likewise expanded the specific fuel consumption of the mustard oil biodiesel [32]. So the chamber pressure is expanded with increment in the MB biodiesel mix. The most extreme pressure of MB 20 fuel was 8.4% more than that of the diesel and furthermore the most elevated pinnacle pressure created among the mixes. The maximum pressure observed for MB20 with 15% EGR was found to 1.9% lesser than that of the diesel. It is due to the presence of exhaust gas in the mixture which reduced the cylinder pressure by decreasing the heat release rate.

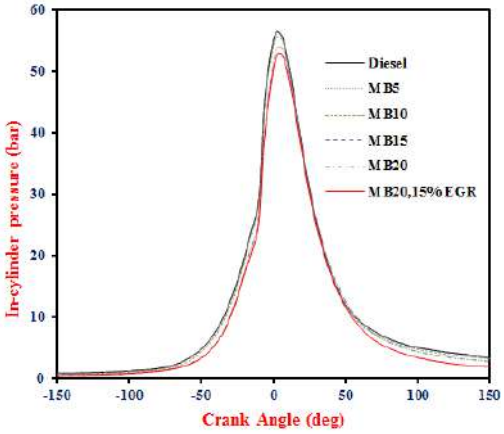

Fig. 7: Cylinder Pressure w.r.t Crank Angle

[Fig. 8] shows the Heat discharge pace of Diesel was higher than the biodiesel mix. This is a result of the higher calorific estimation of diesel contrasted with that of the MB mix. The reduction of about 8.8% and 18.45% of HRR was observed for the MB20 blend and MB20 with 15%EGR. Also the MB20 with 15% EGR have the lesser heat release rate of all the blends as it have the lesser calorific value [33, 34]. Thus the calorific value of the fuel plays a major role in the heat releasing rate.

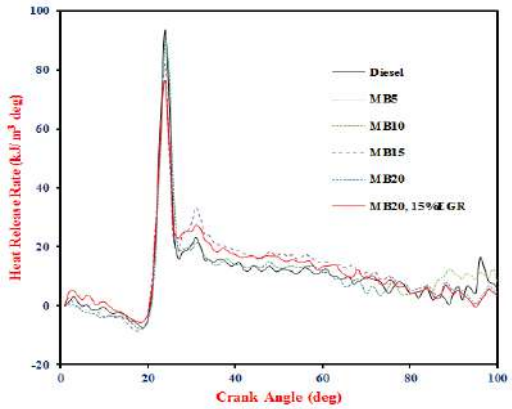

Fig. 8: Heat release rate w.r.t crank angle

IIOAB JOURNAL
ISSN: 0976-3104

CONCLUSION

Subsequently, the mustard biodiesel was arranged and mixed with the diesel in different proportions, it was then tried in a solitary chamber diesel motor. Its performance and effectiveness characters were found. Specific fuel consumption was expanded for all mixes of MB with increment in mixing proportion with DTBP added substance. Brake warm productivity was diminished with increment in the mixing proportion of the fuel with DTBP added substance. HC and CO emissions were diminished with increment in the mixing proportion of the mustard oil biodiesel with DTBP added substance. NOX emission was expanded with increment in the mixing proportion. The impact of the expansion of EGR demonstrates the significant increment and diminishing in specific fuel consumption and brake thermal efficiency individually. The results show that the utilization of mustard oil biodiesel with DTBP added substance will lessen HC and CO however increment NOX emanations. The joined utilization of MB20 with 15% EGR shows decreasing all the discharges from a vehicle. Thus the impact of the DTBP added substance was useful for the decrease of HC and CO discharge however it will build the NOX emanations. Along these lines, the EGR was utilized to lessen all the discharges of the engine.

CONFLICT OF INTEREST

There is no conflict of interest.

ACKNOWLEDGEMENTS

This work was carried out in the Department of Mechanical Engineering, Annamalai University, Chidambaram.

FINANCIAL DISCLOSURE

None.

REFERENCES

[1] Chen J, Bian XQ, Rapp G, Lang J, Montoya A, et al. [2019] From ethyl biodiesel to biolubricants: Options for an Indian mustard integrated biorefinery toward a green and circular economy. Industrial Crops and Products, 137:597-614.

[2] Deep A, Sandhu SS, Chander S. [2017] Experimental investigations on the influence of fuel injection timing and pressure on single cylinder CI engine fueled with 20% blend of castor biodiesel in diesel, Fuel, 210:15-22.

[3] Kumar SAA, Sakthinathan G, Vignesh R, Banu JR, Al-Muhtaseb AH. [2019] Optimized transesterification reaction for efficient biodiesel production using Indian oil sardine fish as feedstock. Fuel, 253:921-929.

[4] Mo B, Chen CQ, Nie H, Jiang YH. [2019] Visiting effects of crude oil price on economic growth in BRICS countries: Fresh evidence from wavelet-based quantile-on-quantile tests. Energy, 178:234-251.

[5] Nabi MN, Rasul MG. [2018] Influence of second generation biodiesel on engine performance, emissions, energy and exergy parameters. Energy Conversion and Management, 169:326-333.

[6] Zeraati-Rezaei S, Al-Qahtani Y, Herreros JM, Ma X, Xu HM. [2019] Experimental investigation of particle emissions from a Dieseline fuelled compression ignition engine, Fuel, 251:175-186.

[7] Haagen smit AJ. [1952] Chemistry and physiology of Los angeles smog, Industrial and engineering chemistry, 44(6):1342-1346.

[8] Ahmad M, Sadia H, Zafar M, Sultana S, Khan MA, Khan Z. [2012] The Production and Quality Assessment of Mustard Oil Biodiesel: A Cultivated Potential Oil Seed Crop. Energy Sources Part a-Recovery Utilization and Environmental Effects, 34(16):1480-1490.

[9] Vlachaos T, Bonnel P, Perujo A, Weiss M, et al. [2014] In-Use Emissions Testing with Portable Emissins Measurement Systems (PEMS) in the Current and Future European Vehicle Emissions Legislation: Overview, Underlying Principles and Expected Benefits, SAE Int J Commer Veh, 7(10):199-215.

[10] Tamilselvan P, Nallusamy N, Rajkumar S. [2017] A comprehensive review on performance, combustion and emission characteristics of biodiesel fuelled diesel engines, Renewable and Sustainable Energy Reviews, 79:1134-1159.

[11] Cenk S, Ahmet NO, Mustafa C. [2010] The influence of operating parameters on the performance and emissions of a DI diesel engine using methanol-blended-diesel fuel, Fuel. 89:1407–1414.

[12] Rafia A, Mohd NH, Noor AI. [2003] Review of air pollution and health impacts in Malaysia, Environmental Research, 92:71–77

[13] Ahmad M, Zafar M, Rashid S, Sultana S, Sadia H, Khan M A. [2013] Production of Methyl Ester (Biodiesel) From Four Plant Species of Brassicaceae: Optimization of the Transesterification Process. International Journal of Green Energy, 10(4):362-369.

[14] Al-dobouni IA, Fadhil AB, Saeed IK. [2016] Optimized alkali-catalyzed transesterification of wild mustard (Brassica juncea L). seed oil. Energy Sources Part a-Recovery Utilization and Environmental Effects, 38(15): 2319-2325.

[15] Antova GA, Angelova-Romova MI, Petkova ZY, Teneva OT, Marcheva MP. [2017] Lipid composition of mustard seed oils (Sinapis alba L). Bulgarian Chemical Communications, 49:55-60.

[16] Boateng AA, Mullen CA, Goldberg NM. [2010] Producing Stable Pyrolysis Liquids from the Oil-Seed Presscakes of Mustard Family Plants: Pennycress (Thlaspi arvense L.) and Camelina (Camelina sativa). Energy & Fuels, 24:(12): 6624-6632.

[17] Chakraborty R, Das S, Bhattacharjee SK. [2015] Optimization of biodiesel production from Indian mustard oil by biological tri-calcium phosphate catalyst derived from turkey bone ash. Clean Technologies and Environmental Policy, 17(2):455-463.

[18] Chakraborty R, Das S, Pradhan P, Mukhopadhyay P. [2014] Prediction of Optimal Conditions in the Methanolysis of Mustard Oil for Biodiesel Production Using Cost-Effective Mg-Solid Catalysts. Industrial & Engineering Chemistry Research, 53(51):19681-19689.

[19] Devarajan Y, Munuswamy DB, Nagappan B, Pandian AK. [2018] Performance, combustion and emission analysis of mustard oil biodiesel and octanol blends in diesel engine. Heat and Mass Transfer, 54(6):1803-1811.

[20] Devarajan Y, Munuswamy DB, Radhakrishnan S, Mahalingam A, Nagappan B. [2019] Experimental Testing and Evaluation of Neat Biodiesel and Heptanol Blends in Diesel Engine. Journal of Testing and Evaluation, 47(2):987-997.

[21] Eryilmaz T, Ogut H. [2011] The effect of the different Mustard oil biodiesel blending ratios on diesel engines performance. Energy Education Science and Technology Part a-Energy Science and Research, 28(1):169-180.

[22] Ganesan S, Rathinam S, Sajin JB, Yuvarajan D. [2019] Performance and emission study on the effect of oxygenated additive in neat biodiesel fueled diesel engine. Energy Sources Part a-Recovery Utilization and Environmental Effects, 41(16):2017-2027.
[23] Gobinath S, Senthilkumar G, Beemkumar N. [2019] Air nanobubble-enhanced combustion study using mustard biodiesel in a common rail direct injection engine. Energy Sources Part a-Recovery Utilization and Environmental Effects, 41(15):1809-1816.
[24] Herfatmanesh MR, Attar MA, Zhao H. [2013] Simultaneous imaging of diesel spray atomization and evaporation processes in a single-cylinder CR diesel engine. Experimental Thermal and Fluid Science, 50:10-20.
[25] Madheshiya AK, Vedrtnam A. [2018] Energy-exergy analysis of biodiesel fuels produced from waste cooking oil and mustard oil, Fuel, 214:386-408.
[26] Mahalingam A, Munuswamy DB, Devarajan Y, Radhakrishnan S. [2018] Investigation on the emission reduction technique in acetone-biodiesel aspirated diesel engine. Journal of Oil Palm Research, 30(2):345-349.
[27] Pandian AK, Munuswamy DB, Radhakrishana S, Ramakrishnan RBB, Nagappan B, Devarajan Y. [2017] Influence of an oxygenated additive on emission of an engine fueled with neat biodiesel. Petroleum Science, 14(4):791-797.
[28] Sanjid A, Masjuki HH, Kalam MA, Rahman SMA, Abedin MJ, Palash SM. [2013] Impact of palm, mustard, waste cooking oil and Calophyllum inophyllum biofuels on performance and emission of CI engine. Renewable & Sustainable Energy Reviews, 27:664-682.
[29] Sastry GSR, Murthy A, Prasad PR, Bhuvaneswari K, Ravi PV. [2006] Identification and determination of bio-diesel in diesel. Energy Sources Part a-Recovery Utilization and Environmental Effects, 28(14):1337-1342.
[30] Singh B, Kaur J, Singh K. [2010] Production of Biodiesel From Used Mustard Oil and Its Performance Analysis in Internal Combustion Engine. Journal of Energy Resources Technology-Transactions of the Asme, 132(3).
[31] Uyumaz A. [2018] Combustion, performance and emission characteristics of a DI diesel engine fueled with mustard oil biodiesel fuel blends at different engine loads. Fuel, 212:256-267.
[32] Yuvarajan D, Babu MD, BeemKumar N, Kishore PA. [2018] Experimental investigation on the influence of titanium dioxide nanofluid on emission pattern of biodiesel in a diesel engine. Atmospheric Pollution Research, 9(1):47-52.
[33] Yuvarajan D. Ramanan MV. [2016] Effect of Magnetite Ferro fluid on the Performance and Emissions Characteristics of Diesel Engine Using Methyl Esters of Mustard Oil. Arabian Journal for Science and Engineering, 41(5):2023-2030.
[34] Yuvarajan D. Ramanan MV. [2016] Experimental analysis on neat mustard oil methyl ester subjected to ultra-sonication and microwave irradiation in four stroke single cylinder Diesel engine. Journal of Mechanical Science and Technology, 30(1):437-446.

ARTICLE

GENOTYPE CATALOGIZATION OF BRUCELLA STRAINS

Evgeny Semenovich Sleptsov[1], Nikolay Vasilievich Vinokurov[1, 2*], Vladimir Gavrilievich Osipov[1], Ivan Vladimirovich Alferov[1], Ayaal Alekseevich Ivanov[2]

[1]*Yakut Research Institute of Agriculture named after M.G. Safronov, 23/1 Bestuzhev-Marlinsky Street, Yakutsk, 677001, RUSSIA*

[2]*Yakutsk State Agricultural Academy, 3 Sergelyakhskoye Shosse 3 km, Yakutsk, 677007, RUSSIA*

ISSN 0976-3104

ABSTRACT

Background: Brucellosis is an infectious disease caused by bacteria of the Brucella genus, which infects almost all types of agricultural and many species of wild animals, as well as humans. Recently, molecular genetic methods for the diagnosis of brucellosis have been introduced into veterinary practice, which allow detecting bacterial DNA in biological material. Methods: A commercial kit of reagents Sileks MagNA-G (Sileks, Russia) based on the method of fixing nucleic acid on magnetic particles, was used for DNA isolation. Results and conclusion: The PCR analysis with primers from the AMOS system confirmed the identification of the currently existing B. melitensis biovars, three biovars of B. abortus, and B. ovis and B. suis species by classical methods. BrA, BAbor, WboA, and Eri primers allowed differentiation of B. abortus at the generic and species levels, as well as identification of B. abortus strain 19 from material taken from experimentally infected animals. Thus, the data obtained on the molecular genetic identification of the DNA of different species of Brucella will largely allow solving the problem of diagnosing brucellosis in animals.

KEY WORDS
Brucellosis, infection process, immunity, strain, genotype, vaccine, biovar

INTRODUCTION

Brucellosis is an infectious disease caused by bacteria of the *Brucella* genus, which infects almost all types of agricultural and many species of wild animals, as well as humans. The infectious agent, which easily migrates from animals to humans, causes acute febrile illness (*B. abortus* - undulating fever, or *B. melitensis* - Maltese fever) and can progress to a chronic form leading to serious complications affecting the musculoskeletal and other body systems. In the system of anti-Brucellar measures, diagnosis is of great importance. Over the years, a large number of diagnostic agents and methods have been tested in experimental and production conditions. The duration of development and decrement of immunobiological responses and their diagnostic value in various animal species have been studied. Recently, molecular genetic diagnostic methods for the diagnosis of brucellosis have been introduced into veterinary practice. These methods detect the DNA of bacteria in biological material and are highly sensitive, specific, fairly simple, and fast (in terms of obtaining the result). One of them is PCR (polymerase chain reaction). Due to its high sensitivity, specificity and universality, the PCR method is increasingly used for the diagnosis of infectious diseases. PCR detects DNA from pathological material containing less than 100 *Brucella* cells. Molecular genetic identification of DNA of different *Brucella* strains allows solving the problem of diagnosis of brucellosis in a substantial way [1-7].

The study aimed to determine the pathogens of brucellosis and identify them in the organs and tissues of experimentally infected animals.

Received: 22 May 2020
Accepted: 12 July 2020
Published: 31 July 2020

MATERIALS AND METHODS

The study was conducted based on the laboratory of chronic infections and the laboratory of molecular biology and biotechnology of the Vyshnevolotsky branch of the All-Russian Institute of Experimental Veterinary on the Lisy island. Clinical, microbiological, serological, and molecular genetic methods proposed by the Joint FAO/WHO Expert Committee on Brucellosis were used. The following equipment was used: laminar-flow cabinets, regular and carbon dioxide thermostats, refrigeration cabinets, deep-freeze cabinets, centrifuges, autoclaves, light microscopes, equipment for freeze-drying, sterilizing filtration, and ultrafiltration.

Oligonucleotide primers for genus-specific and species-specific differentiation of *B. abortus*

DNA purification was conducted using a commercial reagent kit Sileks MagNA-G (Sileks, Russia), which is based on the method for purification of nucleic acids using magnetic particles. BrA primers were used for genus-specific identification of *B. abortus*. *B. abortus* was differentiated from other *Brucella* strains using BAbor oligonucleotides. Further identification of *B. abortus* strain 19 was carried out using primers Eri and WboA [Table 1].

The 25 µl reaction mixture consisted of 10 µl PCR buffer, 3 mmol MgCl, 0.2 mmol dNTPs, 0.4 µmol of each primer, 2.5 units/100 µl of Taq-polymerase, and 10 µl of DNA.

***Corresponding Author**
Email:
nikolaivin@mail.ru

PCR was carried out using the programmable thermal cycler Tertsik (DNA-technology, Russia) according to the following program: 95°C for 10 sec, 61/60/63/65°C (BrA/BAbor/Eri/WboA) for 10 sec, and 72°C for 10 sec; 40 cycles, with two-minute preliminary denaturation at 95°C and subsequent three-minute elongation at 72°C.

Table 1: Characteristics of oligonucleotide primers for the genus-specific and species-level differentiation of *B. abortus*

Primer	5'-3' sequence	Length, n	Amplicon size, bp	Annealing point, °C
BrA-F	AGTCAGACGTTGCCTATT	18	260	61
BrA-R	GTGTTCAGCCTTGATATG	19		61
BAbor-F	GTTCTTGCTGGTCTTGCGGTG	21	1054	60
BAbor-R	AGCGCAGGAGATGCAGGCAC	20		60
Eri-F	GCGCCGCGAAGAACTTATCAA	21	178	63
Eri-R	CGCCATGTTAGCGGCGGTGA	20		63
WboA-F	GCCAACCAACCCAAATGCTCACAA	26	400	65
WboA-R	TTAAGCGCTGATGCCATTTCCTTCAC	24		65

Oligonucleotide primers in the AMOS system

AMOS (*abortus*, *melitensis*, *ovis*, and *suis*) method proposed by Bricker et al. was used to identify *B. melitensis* (all biovars), *B. ovis*, first, second, and fourth biovars of *B. abortus* and *B. suis*. The method is based on species-specific or biovar-specific characteristics of the localization of the genetic element IS711 in the chromosomal DNA of *Brucella*. For identification, five primers were used. One of them is specific to the sequence of genetic element IS711. Other four are specific to adjacent DNA sequences, which are characteristic of each type of *Brucella* [Table 2].

The 25 µl reaction mixture consisted of 10 µl PCR buffer, 2.2 mmol MgCl, 0.2 mmol dNTPs, 0.4 µmol of each primer, 2.5 units/100 µl of Taq-polymerase, and 10 µl of DNA.

PCR was carried out using the programmable thermal cycler Tertsik (DNA-technology, Russia) according to the following program: 94°C for 20 sec, the primer annealing temperature ranged from 56.5°C to 60°C, and the primers annealed on the matrix for 20 sec, elongation at 72°C for 40 sec; 35 cycles.

Table 2: Characteristics of the oligonucleotide primers of the AMOS system

Brucella	5'-3' sequence	Direction	Length, n	Amplicon size, bp	Annealing point, °C
B. abortus	GACGAACGGA ATTTTTCCAATCCC	forward	24	498	55.5
	TGCCGATCACT TAAGGGCCTTCAT	reverse	24		56.5
B. ovis	CGGGTTCTG GCACCATCGTCG	forward	21	976	56.0
	TGCCGATCACT TAAGGGCCTTCAT	reverse	24		56.5
B. melitensis	AAATCGCGTC CTTGCTGGTCTGA	forward	23	731	56.0
	TGCCGATCACT TAAGGGCCTTCAT	reverse	24		56.5
B. suis	GCGCGGTTTTC TGAAGGTTCAGG	forward	23	285	55.0
	TGCCGATCACT TAAGGGCCTTCAT	reverse	24		56.5

The amplification results were analyzed using horizontal electrophoresis in 2% agarose gel. 100 bp Ladder DNA Marker (100bp-3000bp) (Axygene, USA) was used as a molecular mass marker.

Cataloging of genotypes of *Brucella* strains from the collection of pathogenic and vaccine strains

Brucella strains in the collection of pathogenic and vaccine strains were studied based on biochemical, serological, and virulent properties. The study considered the ability of *Brucella* to release H2S, the need for CO2 during cultivation, sensitivity to erythritol and aniline dyes (fuchsin, thionin), the dissociation degree in samples with trypaflavine, acriflavin and miostagmic reaction, the color of the grown White Wilson colonies, and the ability to grow in the presence of penicillin antibiotics. “A” and “M” antigenic structures of *Brucella* were determined using monoreceptor serum. Sensitivity to a specific bacteriophage was also studied. Virulent properties were studied in laboratory animals; the infection index and antigenic and allergenic properties were determined. As a result, the current species affiliation existing strains was

IIOAB JOURNAL
ISSN: 0976-3104

confirmed. Thirty-six strains belong to strain *B. melitensis*, 77 strains belong to *B. abortus*, 25 belong to *B.ovis*, 53 strains belong to *B. suis*, one strain belongs to *B. neotomae*, and two strains belong to *B. canis*.

For the genus-specific and species-level differentiation of *B. abortus* and for the identification of *B. abortus* 19 strain, we used primers that can be applied in the molecular genetic diagnosis of brucellosis in infected animals.

RESULTS AND DISCUSSION

The BrA primers [Table 1] were synthesized based on the BCSP31 gene sequence. This sequence is identical for all types of *Brucella* and therefore, these primers are genus-specific. As a result of PCR, a specific fragment of 260 bp was amplified [Fig. 1]. This sequence is identical for all types of *Brucella* and therefore, these primers are genus-specific. As a result of PCR, a specific fragment of 260 bp was amplified [Fig. 1].

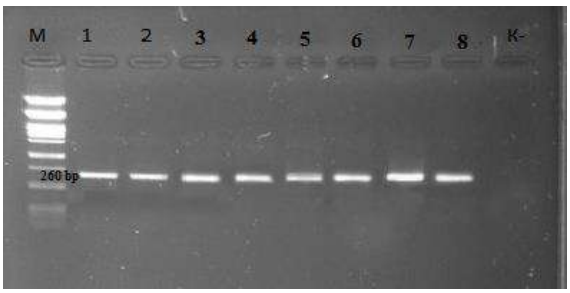

Fig. 1: Results of testing of the effectiveness of BrA primers. Designations: M – DNA marker; 1 – retropharyngeal right lymphnode; 2 – inguinal left lymphnode; 3 – mediastinal lymphnode; 4 – liver; 5 – spleen; 6 – *B. abortus* 19; 7 – *B. abortus* 54; 8 – *B. melitensis* H-102; K- – negative test control

Differentiation of *B. abortus* from other *Brucella* strains is possible due to the absence of a 25 kb region in the chromosomal DNA of all *B. abortus* biovars. PCR was carried out using BAbor oligonucleotides [Table 1], which hybridize with DNA sequences that flank the 25 kp region during annealing. This region is present in all species of *Brucella* except *B. abortus*. A fragment of 1054 bp was amplified for *B. abortus*, and for the remaining species of *Brucella*, amplification did not take place, because the required fragment length was very large (26 kp). [Fig. 2] shows the results of PCR with BrA primers. The amplicon size in the presence of *B. abortus* DNA in the sample was 1054 bp.

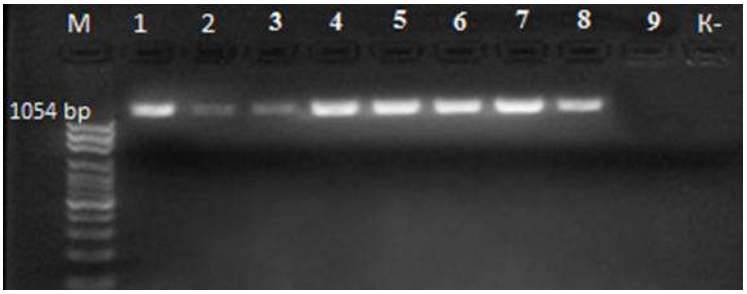

Fig. 2: Results of testing of the effectiveness of BAbor primers. Designations: M – DNA marker; 1 – retropharyngeal right lymphnode; 2 – inguinal left lymphnode; 3 – mediastinal lymphnode; 4 – liver; 5 – spleen; 6 – *B. abortus* 19; 7 – *B. abortus* 54; 8 – popliteal right lymphnode; 9 – *B. melitensis* H-102; K- – negative test control

The identification of *B. abortus* 19 was based on the absence of a 702 bp fragment in the Eri locus. Oligonucleotides were selected in such a way that one of them annealed at the Eri locus common for strain 19, *B. abortus* strains, and other species, while the WboA annealed at the gene that is absent in strain 19. When performing PCR with WboA primers and DNA of all *Brucella* strains (including strain 19), a specific 400 bp fragment was amplified. When performing PCR with the same material and Eri primers, a 178 bp fragment was amplified for all *Brucella* strains, with the exception of strain 19. Using these primers in parallel allowed us to identify *B. abortus* strain 19 [Fig. 3].

From the PCR results presented in [Table 3], it can be seen that the primers BrA, BAbor, WboA, and Eri allowed differentiating *B. abortus* at the generic and species levels and identifying *B. abortus* strain 19 in the material taken from experimentally infected animals.

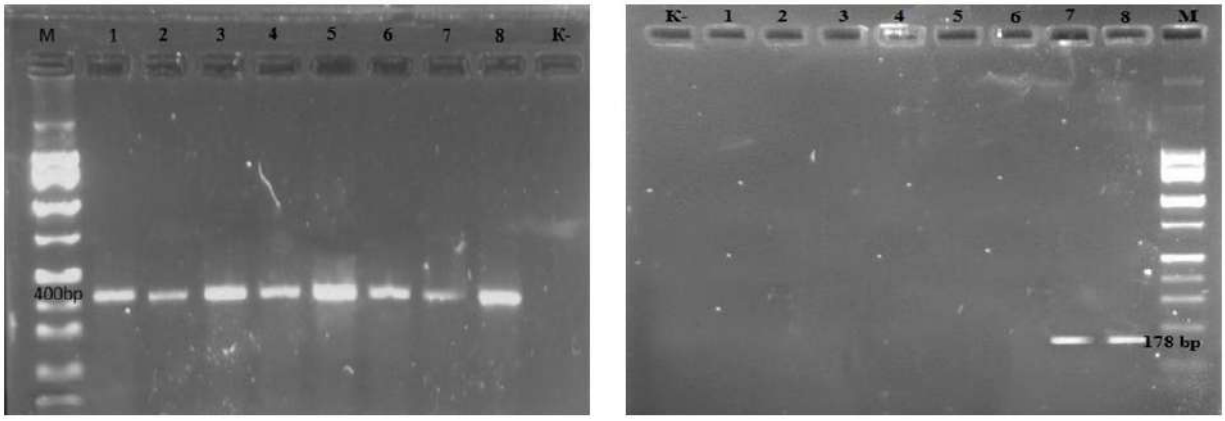

Fig. 3: Results of testing of the effectiveness of WboA (left) and Eri (right) primers. Designations: M – DNA marker; 1 – retropharyngeal right lymphnode; 2 – inguinal left lymphnode; 3 – mediastinal lymphnode; 4 – liver; 5 – spleen; 6 – *B. abortus* 19; 7 – *B. abortus* 54; 8 – *B. melitensis* H-102; K- – negative test control.

Table 3: Results of PCR with primers BrA, BAbor, WboA, and Eri (number of positive samples /total number of samples)

Material	Primers			
	BrA	BAbor	WboA	Eri
Retropharyngeal right lymphnode	4/4	4/4	4/4	0/4
Retropharyngeal left lymphnode	4/4	4/4	4/4	0/4
Inguinal right lymphnode	4/4	3/4	4/4	0/4
Inguinal left lymphnode	4/4	4/4	4/4	0/4
Popliteal right lymphnode	4/4	4/4	4/4	0/4
Popliteal left lymphnode	4/4	3/4	4/4	0/4
Mediastinal lymphnode	4/4	4/4	4/4	0/4
Paraaortal right lymphnode	3/3	3/3	3/3	0/3
Paraaortal left lymphnode	3/3	3/3	3/3	0/3
Antescapular left lymphnode	4/4	4/4	4/4	0/4
Spleen	4/4	4/4	4/4	0/4
Kidneys	4/4	4/4	4/4	0/4
Liver	4/4	4/4	4/4	0/4
Suspension of *B. abortus* 19	+	+	+	-
Suspension of *B. abortus* 54	+	+	+	+
Suspension of *melitensis* H-102	+	-	+	+

PCR was performed using five primers of the AMOS system, one of which is specific to the IS711 sequence, and the other four are specific to adjacent DNA regions specific for each *Brucella* species. When testing strains of *B. melitensis*, *B. ovis*, and *B. suis*, specific fragments of 731 bp, 976 bp, and 285 bp were amplified, respectively. The specific product of PCR analysis of *B. abortus* was 498 bp [Fig. 4].

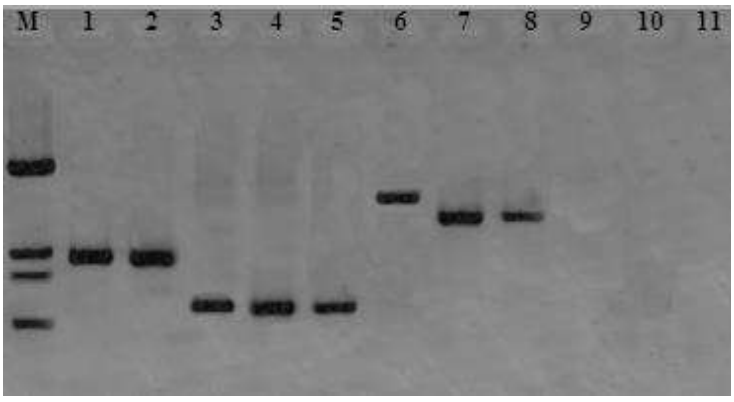

Fig. 4: Results of testing of the effectiveness of AMOS primers. Designations: M – DNA marker; 1 – *B. abortus* 19; 2 – *B. abortus* 54; 3 – *B. suis* HH-1; 4 – *B. suis* 002; 5 – *B. suis* 245; 6 – *B. ovis* 63/91; 7 – *B. melitensis* H-102; 8 – *B. melitensis*; 9 – *B. neotomae* 66/2; 10 – *B. canis* 6/66; 11 – negative test control.

Thus, the obtained PCR data with primers BrA, BAbor, WboA, Eri in each *Brucella* species with corresponding fragment sizes are similar to data of other authors [1, 7].

IIOAB JOURNAL
ISSN: 0976-3104

CONCLUSION

We performed the catalogization of *Brucella* strain genotypes from a collection of pathogenic and vaccine strains of causative agents of animal infectious diseases of the All-Russian Institute of Experimental Veterinary.

In the study of *Brucella* cultures from the collection of pathogenic and vaccine strains of causative agents of animal infectious diseases of the All-Russian Institute of Experimental Veterinary the cultures were attributed to species using cultural-biochemical, tinctorial, and serological methods. Thirty-six strains belong to *B. melitensis*, 77 strains belong to *B. abortus*, 25 strains belong to *B. ovis*, 53 strain belong to *B. suis*, one strain belongs to *B. neotomae*, and two strains belong to *B. canis*. PCR analysis with the use of primers from the AMOS system confirmed the identification of currently existing biovars of *B. melitensis*, three biovars of *B. abortus*, species *B. ovis* and *B. suis* using classical methods. Primers BrA, BAbor, WboA, and Eri allowed differentiating *B. abortus* at the generic and species levels, as well as identifying *B. abortus* strain 19 in the material taken from experimentally infected animals. Consequently, the data of the molecular genetic identification of DNA of different *Brucella* species will significantly simplify the solution to the problem of diagnosing animal brucellosis.

CONFLICT OF INTEREST

The authors declare no competing interests in relation to the work.

ACKNOWLEDGEMENTS

None.

FINANCIAL DISCLOSURE

None.

REFERENCES

[1] Albertyan MP, Iskandarov MI, Fedorov AI. [2013] Immunobiologicheskie svoistva slaboagglyutinogennoi vaktsiny protiv brutselleza selskokhozyaistvennykh zhivotnykh [Immunobiological characteristics of weakly agglutinogenic vaccines against brucellosis of livestock animals]. Veterinariya i kormlenie [Veterinary and feeding], 4:20-23.

[2] Fedorov AI, Iskandarov MI, Ignatov PE, Al'bertyan MP, Nestrelyaev SS, Nekrasov AV, Khaitov RM, Petrov RV. [2006] Znachenie gumoralnogo i kletochnogo immuniteta pri brutselleze [The importance of humoral and cellular immunity in brucellosis]. Physiology and pathology of the immune system, 10(8):3-7.

[3] Fedorov VI, Sleptsov ES, Vinokurov NV, Grigoriev II, Zakharova OI, Maksimova AN. [2018] On Adapting Domestic Even Reindeer to the Mountain-Taiga Zone of The North-East of Russia. Journal of Pharmaceutical Sciences and Research, 10(7):1660-1662.

[4] Fedorov VI, Stepanov AI, Sleptsov ES, Vinokurov NV, Bochkarev II, Maksimova AN. [2018] Northern Domestic Reindeer Husbandry of the Republic of Sakha (Yakutia): Retrospective Analysis and Development Trends. Journal of Pharmaceutical Sciences and Research, 10(10):2559-2563.

[5] Godfroid J. [2017] Brucellosis in livestock and wildlife: zoonotic diseases without pandemic potential in need of innovative one health approaches. Archives of Public Health, 75(1):34.

[6] Kanouté YB, Gragnon BG, Schindler C, Bonfoh B, Schelling E. [2017] Epidemiology of brucellosis, Q fever and Rift Valley fever at the human and livestock interface in northern Côte d'Ivoire. Acta tropica, 165:66-75.

[7] Vinokurov NV, Sleptsov ES, Stepanov AI, Fedorov VI, Robbek NS, Dayanova GI, Ivanov AA. [2019] Testing the biological properties of the vaccine from strain Brucella abortus 75/79-AB on reindeer. Advances in Animal and Veterinary Sciences, 7(S1):40-44.

IIOAB JOURNAL

ARTICLE

EFFECT OF CONIFEROUS ADDITIVE ON PRODUCTIVE AND BIOLOGICAL PARAMETERS OF COWS

Tamara Fiodorovna Lefler[1], Lilia Evgenyevna Tyurina[1], Viktor Anatolyevich Ryzhov[2*], Vasily Pavlovich Korotky[2], Nikolay Petrovich Buryakov[3], Maria Alekseyevna Buryakova[3]

[1]Federal State Budgetary Educational Institution of Higher Education "Krasnoyarsk State Agrarian University", 90 Mira St., Krasnoyarsk, 660049, RUSSIA

[2]Science and Technology Center "Khiminvest", 6/1 Nizhne-Volzhskaya Naberezhnaya, Nizhny Novgorod, 603001, RUSSIA

[3]Federal State Budgetary Educational Institution of Higher Education "Russian Timiryazev State Agrarian University", 49 Timiryazevskaya St., Moscow, 127550, RUSSIA

ISSN 0976-3104

ABSTRACT

The article presents the results of studying the effect of the coniferous energy additive on fodder palatability, milk yield and quality, and reproductive ability of cows. The experiment has been performed in the conditions of the Mikhailovskoye Federal State Unitary Enterprise in the Uzhur district of the Krasnoyarsk Krai and at the Krasnoyarsk State Agrarian University. The research has been aimed at studying the effect of the coniferous energy additive on the productive and biological parameters of cows. It has been found that the use of the coniferous energy feed additive in the diets has contributed to the better fodder palatability by the cows in experimental groups III and IV (the metabolic energy concentration has been 11.26 – 11.44 MJ/kg). The cows in the experimental groups have exceeded their peers in the reference group both in terms of the daily produced amount of milk (by 0.6 – 6.8 kg) and in general throughout the experiment (by 56 – 676 kg), P<0.05; P<0.01. The same cows also produced more milk fat and protein by 28.1 – 23.7 and 21.9 – 19.0 kg. The feed additive has contributed to the reduction of the duration of the service period and the conception rate.

KEY WORDS
coniferous energy additive, black-motley breed, hemoglobin, erythrocytes, conception rate, service period

INTRODUCTION

The constant growth of the prices of raw materials makes specialists search for the ways of reducing the cost of fodder, which, as known, accounts for 70 % in the structure of the livestock breeding product costs, and, despite the growth of productivity and the reduction of production costs in physical terms, remains high in monetary terms.

In the conditions of intensifying the livestock production, creating a strong and balanced fodder base plays a decisive role in the successful growth of production. A strong fodder base is determined by both the total fodder production and its quality. Both indicators equally determine the efficiency of dairy cattle breeding. In this respect, a necessity arises to search for and introduce new methods and techniques in the production of animal fodder. One of the ways of reducing the production costs in monetary terms is reducing the formulation costs through the use of various feed additives. The alternatives are nontraditional feed additives obtained from the timber processing wastes and byproducts (branches and treetops, bark, lily pads, chemical processing wastes) that contribute to normalizing the physiological processes, increasing the productivity, and preserving the livestock [1-3].

Received: 27 May 2020
Accepted: 23 July 2020
Published: 9 Aug 2020

In the Krasnoyarsk Krai, 50.5 % of the reserves of ripe and overripe siberian fir (*Abies sibirica*) suitable for use are located. The fir reserves amount to 1,296.6 million m3, or 9.3 % of the reserves of all wood species [4]. The composition of the natural coniferous extract is close to that of the natural cellular fluid in the needles, but the concentration of the water-soluble substances in it is lower. The composition of sugars in the coniferous extract is dominated by glucose, which accounts for almost 30 % of the total amount of monosaccharides. The content of mannose in the spruce water extract is 16 %, in the pine water extract — 9 %; the content of oligosaccharides is 13 – 15 %. The literature data indicate the presence of sucrose, melibiose, and a significant amount of maltose in the needles (up to 20 %). Among macroelements, nitrogen, phosphorus, potassium, iron, sodium are found, and among microelements, manganese, cobalt, copper, zinc are defined. The presence of these and other elements enhances the nutritional value of water extracts and activates physiological and biochemical processes in the body of animals [5, 6].

The employees of the Khiminvest Scientific-Technical Center LLC (Nizhny Novgorod) have developed a technology for processing the needles of coniferous wood species, which is based on extracting biologically active substances with the use of a new selective extractant. A coniferous energy feed additive with improved properties that ensure the long-term preservation of its consumer qualities has been created [7, 8].

***Corresponding Author**
Email:
woodnn@yandex.ru

This research has been aimed at studying the effect of the coniferous energy additive (CEA) on the productive and biological parameters of cows in the conditions of the Krasnoyarsk Krai.

IIOAB JOURNAL
ISSN: 0976-3104

MATERIALS AND METHODS

The studies for determining the effect of the CEA on milk productivity and reproductive ability were performed from September to December 2019, in the conditions of the Mikhailovskoye Federal State Unitary Enterprise in the Uzhur district of the Krasnoyarsk Krai and at the Department of Zootechnics and Cattle Breeding Products Processing of the Institute of Applied Biotechnology and Veterinary Medicine at the Krasnoyarsk State Agrarian University (the protocol was approved by the institute's council No. 2 dated October 24, 2019), with four groups of black-motley cows, 10 animals in each. Reference group I was formed from the cows that received the fodder of in-house production according to the detailed norms of the Federal Science Center for Animal Husbandry [9]. The cows in the experimental groups, in addition to the main diet, received the CEA as part of the concentrated fodder according to the following scheme [Table 1].

Table 1: The scheme of the scientific and practical experiment

Group	Feeding conditions	Studied indicators
Reference group I	Main diet (MD)	1 – Consumption of fodder and nutrients 2 – Milk productivity of the cows 3 – Reproductive ability
Experimental group II	MD + 100 g of the CEA	
Experimental group III	MD + 150 g of the CEA	
Experimental group IV	MD + 200 g of the CEA	

The experiment lasted for 130 days in the autumn-and-winter period. The cows were kept in the same conditions.

The coniferous energy feed additive was a uniform viscous pasty mass with a coniferous smell that contained 50 % of glycerol and 50 % of the product ecologically obtained from needles. In the organisms of newly-calved cows, glycerin is easily absorbed in the gastrointestinal tract and becomes a good material for the intermediate metabolism as a gluco-plastic component for glucose synthesis and providing energy for the animal. The phyto component, the needles, is the source of vitamins, amino acids, micro- and macro elements, and various biologically active substances with a positive effect on the organisms of calved cows [10].

Biometric processing of the results of the experiment was carried out using a personal computer in the Microsoft Excel program with the calculation of arithmetic mean values and corresponding errors (M ± m). The significance of the differences between the compared indicators in groups was assessed by the Student's t-test with the following significance levels: * - P <0.05; ** - P <0.01; *** - P <0.001 [11].

RESULTS AND DISCUSSION

Accounting for the fodder consumption allowed to determine the metabolic energy concentrations in the diets of the compared groups of cows; these concentrations did not differ significantly and amounted to 11.26 – 11.44 MJ per kilogram of dry weight. The sugar to protein ratio (0.90 – 0.95) and the calcium to phosphorus ratio (1.90:1.0, 1.98:1.0) corresponded to the physiological needs of the cows during the milking period.

Milk productivity and milk composition are determined by the genetic parameters and the feeding and keeping conditions. The authors studied the effect of the coniferous energy feed additive on milk productivity in the first 100 days of lactation [Table 2].

Table 2: Milk productivity of the cows over 100 days of lactation, kg

Indicator	Group			
	I	II	III	IV
Daily milk yield	20.6 ± 1.53	21.2 ± 1.69	27.4 ± 1.75**	26.4 ± 1.70*
Amount of milk	2,064 ± 68.4	2,120 ± 77.5	2,740 ± 65.9***	2,637 ± 86.5***
Mass fraction of fat, %	3.97 ± 0.04	3.99 ± 0.05	4.01 ± 0.05*	4.00 ± 0.05*
Mass fraction of protein, %	3.34 ± 0.05	3.28 ± 0.04	3.31 ± 0.05	3.33 ± 0.03
Amount of milk fat	81.94 ± 3.66	84.59 ± 3.99	109.87 ± 5.17***	105.47 ± 4.88***
Amount of milk protein	68.94 ± 3.45	69.54 ± 4.20	90.69 ± 5.42**	87.81 ± 4.59***

(Hereinafter, the significance of the difference is shown with respect to the same indicator of the compared control group: *P<0.05; **P<0.01; *** P<0.001)

The cows in the experimental groups were superior to their peers in the reference group both in terms of the daily produced amount of milk (by 0.6 – 6.8 kg) and in general throughout the experiment (by 56 – 676 kg), P<0.05; P<0.01. Over 100 days of lactation, the mass fraction of fat in the milk was also the highest in the cows in groups III and IV; it amounted to 4.01 % and 4.0 %, which was by 0.04 – 0.01 % higher than in their peers. The difference between the indicators of the groups was not reliable. The same cows also produced more milk fat and protein by 28.1 – 23.7 and 21.9 – 19.0 kg, P<0.01; P<0.001. Thus,

IIOAB JOURNAL
ISSN: 0976-3104

introducing the coniferous energy feed additive in the amount of 150 g had the best effect on milk productivity.

No significant difference was found in terms of the main parameters of milk quality (fat and protein mass fractions, total protein, casein, whey proteins, and mineral substances) in the compared groups of cows [Table 3]. The organoleptic assessment of the milk also showed that the samples had no significant differences in their color, smell, texture, or taste.

Table 3: Milk composition and properties

Indicator	Group			
	I	II	III	IV
Mass fraction of fat, %	3.97 ± 0.05	3.99 ± 0.02	4.01 ± 0.05	4.0 ± 0.05
Mass fraction of total protein, %	3.34 ± 0.06	3.28 ± 0.05	3.31 ± 0.04	3.33 ± 0.03
Mass fraction of casein, %	2.65 ± 0.06	2.58 ± 0.07	2.60 ± 0.05	2.62 ± 0.08
Mass fraction of whey proteins, %	0.69 ± 0.03	0.70 ± 0.05	0.71 ± 0.04	0.71 ± 0.03
Mass fraction of lactose, %	4.72 ± 0.03	4.48 ± 0.04***	4.57 ± 0.03	4.75 ± 0.04**
Mass fraction of nonfat milk solids, %	9.08 ± 0.05	8.63 ± 0.06***	8.79 ± 0.04***	9.14 ± 0.04***
Mass fraction of dry matter, %	12.89 ± 0.19	12.46 ± 0.25	12.63 ± 0.21	12.98 ± 0.22
Mass fraction of minerals, %	0.72 ± 0.03	0.69 ± 0.04	0.70 ± 0.03	0.73 ± 0.03
Milk density, kg/m^3	1,030.1 ± 1.25	1,028.3 ± 1.22	1,028.9 ± 1.16	1,030.3 ± 1.23
Energy value, kcal	694.5 ± 4.3	680.2 ± 5.6	688.0 ± 4.7	695.3 ± 4.8

In terms of lactose, nonfat milk solids, and the mass fraction of dry matter in the milk, the cows in group IV insignificantly exceeded their peers by 0.64 – 6.03 % (P<0.01).

In studying the biological value of the milk, no significant difference was noted in terms of the amino acid composition. It was found that the milk of the cows that received the CEA with fodder was a biologically complete product suitable for industrial processing and human nutrition as whole milk.

Reproductive ability of the cows in the herd influences the duration of their practical use. With the degradation of the cows' calf-producing ability, the average interval between calvings usually increases and the duration of the cows' practical use decreases. Therefore, studying cows' reproductive ability in scientific and economic experiments is of great economic importance.

Table 4: Reproductive ability of the cows

Indicator	Group			
	I	II	III	IV
Conception rate	1.22 ± 0.17	1.15 ± 0.12	1.10 ± 0.15	1.13 ± 0.16
Duration of parturition, hour-min	3-25 ± 35.9	3-10 ± 28.7	3-00 ± 26.9	3-00 ± 30.1
Duration of afterbirth expulsion, hour-min	2-25 ± 29.5	2-30 ± 30.0	1-55 ± 29.9*	2-05 ± 30.2
Duration of the service period, days	99.0 ± 14.3	98.0 ± 9.8	94.0 ± 11.2	95.0 ± 15.1

The use of the CEA for feeding down-calvers helped enrich their organisms with a complex of vitamins, amino acids, micro- and macroelements, and various biologically active substances. Therefore, calving and afterbirth expulsion occurred faster in the cows in the experimental groups (P>0.005). The average value of the indicators showed increased reproductive ability, but was not statistically significant. For instance, parturition was 25 and 15 minutes longer in the cows in the reference group than in their peers. No afterbirth retention and other pathological deviations were observed during parturition. However, the best indicators were observed in the experimental groups; the difference was 5 to 30 minutes. Despite the assertion of many scientists [1, 12, 13] that high milk productivity of cows increases the service period and the conception rate, it was not confirmed in the studies of the authors.

CONCLUSION

The use of the coniferous energy feed additive in the diets has contributed to the better fodder palatability by the cows in experimental groups III and IV, which has had an effect on the metabolic energy concentration that has reached 11.26 – 11.44 MJ/kg. The coniferous energy feed additive has had a positive effect on milk productivity. The cows in the experimental groups were superior to their peers in the reference group both in terms of the daily produced amount of milk (by 0.6 – 6.8 kg) and in general throughout the experiment (by 56 – 676 kg), P<0.05; P<0.01. The coniferous energy feed additive helps reduce the duration of the service period and the conception rate, and normalizes the parturition activity.

CONFLICT OF INTEREST

The authors declare no competing interests in relation to the work.

ACKNOWLEDGEMENTS

None.

FINANCIAL DISCLOSURE
None.

REFERENCES

[1] Ernst LK, Naumenko ZM, Ladinskaya SI. [2006] Feed resources of the forest. RAAS, Moscow, 369.
[2] Ammerman C, Baker D, Lewis A. [1995] Bioavailability of Nutrients for Animals. Academic Press, San Diego, 441.
[3] Pfister JA, Villalba JJ, Gardner D. [2012] Effect of dietary protein level and quebracho tannin on consumption of pine needles (Pinus ponderosa) by beef cows. The Professional Animal Scientist, 28(5):528-533.
[4] Kozina EA, Tabakov NI. [2013] The use of the feed additive obtained from timber processing wastes in the diets of lactating cows. Bulletin of the Krasnoyarsk State Agrarian University, 3:116.
[5] Britvina IV, Litvinova NY, Novikov AS. [2018] The effectiveness of using the Avatar energy additive for feeding cows in the transit period. Chief Zootechnician, 10:3-11.
[6] Hill TM, Aldrich JM, Schlotterbeck RL, Bateman II HG. [2007] Apex Plant Botanicals for Neonatal Calf Milk Replacers and Starters. The Professional Animal Scientist, 23(5):521-526.
[7] Korotky VP, Ryzhov VA, Turubanov AI, Roshchin VI, Bajunova EA, et al. [2015] Coniferous energy additive. Patent RU 2543814.
[8] Ryzhov VA, Ryzhova ES, Korotky VP, Yesipovich AL, Kazantsev OA, Zenkin AS. [2014] The coniferous energy feed additive for livestock breeding. Scientific and methodological electronic journal Concept, 26:431-435.
[9] Kalashnikov AP, Fisinin VI, Shcheglov VV, Pervoye NG, Klejmenov NI, Strekozov NI, Bugdayev IE. [2003] The norms and diets for feeding farm animals. Handbook. Ministry of Agriculture of the Russian Federation, Russian Academy of Agricultural Sciences, All-Russian State Research livestock institute, Moscow, RU.
[10] Yurina NA. [2018] Optimization of the feeding of lactating cows. Agricultural science, 9(75):48-51.
[11] Yakovenko AM, Antonenko TI, Selionova MI. [2013] Biometric methods of analysis of qualitative and quantitative characteristics in animal science. Textbook. Agrus, Stavropol, p91.
[12] Zamanbekov NA, Kosh-Kinbay VA, Siyabekov ST. [2018] The effect of the coniferous energy additive (CEA) on some biochemical parameters of dairy cows' blood. In: Actual problems of Veterinary Medicine: Materials for the international scientific-practical conference dedicated to the 90th anniversary of Professor V.A. Kirshin, Federal Center for Toxicological, Radiation and Biological Safety, Kazan, Republic of Tatarstan, Russia, RU
[13] Evglevsky AA, Turnayev SN, Tarasov VY, Lebedev AF, Shvec OM, Evglevskaya EP. [2017] The problems of ensuring the health of high-yielding cows in animal husbandry and practical ways of solving them. Bulletin of the Kursk State Agricultural Academy, 4:26–30.

ARTICLE

IMMUNOGENIC AND ANTIGENIC PROPERTIES OF AGGLUTINOGENIC AND WEAKLY AGGLUTINOGENIC VACCINES AGAINST ANIMAL BRUCELLOSIS

Evgeniy Semenovich Sleptsov[1], Nikolay Vasilievich Vinokurov[1, 2*], Alexandra Innokentievna Pavlova[2], Lena Prokopyevna Koryakina[2], Tatyana Dmitriyevna Rumyantseva[2]

[1]Yakut Research Institute of Agriculture named after M.G. Safronov, 23/1 Bestuzhev-Marlinsky Street, Yakutsk, 677001, Republic of Sakha (Yakutia), RUSSIA

[2]FSBEI HE, Yakutsk State Agricultural Academy, 3 Sergelyakhskoye Shosse 3 km, Yakutsk, 677007, Republic of Sakha (Yakutia), RUSSIA

ISSN 0976-3104

ABSTRACT

Background: *Brucellosis is a particularly dangerous zoonotic disease, widespread in the Russian Federation. The research was aimed at studying the immunogenic and antigenic properties of agglutinogenic and weakly agglutinogenic vaccines against animal brucellosis.* ***Methods:*** *A suspension of brucellae from the Brucella abortus 19 vaccine strain obtained from immune and intact animals had been injected into the tubes with various blood fractions until the final concentration of 1 billion microbial cells was reached. The concentration of brucellae in the bacterial mass was determined according to the optical standard of turbidity and monitored till incubation.* ***Results and Conclusions:*** *The agglutinating and complement-binding antibodies detected in the diagnosis of brucellosis are not essential for brucellosis immunity and mainly play the role of the "witness" of the immune system's contact with the pathogen. Brucellosis immunity is mainly of the cell type, but some precipitin antibodies show the phenomenon of opsonization and blocking the pathogenicity factor, and play a positive role in forming brucellosis immunity. Veracious assessment of the immunogenicity of agglutinogenic and weakly agglutinogenic vaccines against brucellosis is possible only with the use of the direct infestation method.*

KEY WORDS
brucellosis, brucellae, vaccine, strai, antibodies, immunogenicity, immunity, lymphocytes

Received: 24 May 2020
Accepted: 29 July 2020
Published: 17 Aug 2020

***Corresponding Author**
Email:
nikolaivin@mail.ru

INTRODUCTION

Brucellosis is an infectious disease caused by bacteria of the *Brucella* genus, which infects almost all types of agricultural and many species of wild animals, as well as humans. The infectious agent, which easily migrates from animals to humans, causes acute febrile illness (*B. abortus* - undulating fever, or *B. melitensis* - Maltese fever) and can progress to a chronic form leading to serious complications affecting the musculoskeletal and other body systems.

In recent years, immunology has significantly advanced in studying the morphology and functions of various lymphocyte subpopulations and the mechanisms of their cooperation. As a consequence, the extreme titer of specific antibodies, or the number of antibody-forming cells, is sometimes considered as a key quantitative indicator of the immune status of the organism, which, however, does not always coincide with the results of experimental infestation.

In several experiments devoted to studying brucellosis immunity, the authors observed a clear lack of correlation between the titer of the antibodies detected in AT and CFT with the standard diagnostic and the state of immunity in guinea pigs, which was checked by experimental infestation. These data are consistent with the works of many researchers. Since the 40ies of the 20th century, reports have been published stating that high titer of antibodies does not guarantee protection for the animals from experimental infestation [1-3].

In veterinary medicine, therapeutic serums are widely and successfully used against many bacterial and viral infections. This also raises the possibility of the essential role of antibodies against the brucellosis infection. There is no such serum against brucellosis, although, in the 20th century, many authors tried to develop it and even obtained some positive results. In their studies with guinea pigs, the authors also injected the anti-brucellosis serum obtained by hyper immunization of rabbits with the brucellosis vaccine to the experimental animals immediately after infestation, and three more times at five to six days' intervals. The bacteriological study a month after infestation and treatment with the anti-brucellosis serum revealed 63 % of the experimental animals that were free from the brucellosis infection with 100 % infestation of the reference animals. Analyzing the materials of the developments in this area, it may be noted that in vivo, the preventive property of the immune anti-brucellosis serum was manifested, but only if the serum had been introduced before or simultaneously with the infecting culture. In the period of developed infection, the serum did not possess any preventive properties. Apparently, given the intracellular nature of the parasitism of *brucellae*, the cell membrane created a reliable barrier for the humoral bactericidal blood factors.

The body's defense against the brucellosis infection is determined by cellular immunity: after phagocytosis of the *brucellae*, macrophages transmit information to the T-lymphocytes responsible for cellular immunity.

IIOAB JOURNAL
ISSN: 0976-3104

In this process, some antibodies, such as precipitin or bactericidal antibodies play a useful role. On the contrary, agglutinating antibodies (or agglutinins) are passive witnesses of the organism's contact with the *brucellae*. However, the authors note that a vaccine from a mutated *brucellae* strain in the R-form (of the Brucella abortus 45/20 type) induces exclusively cellular protection. In this case, a non agglutinogenic vaccine is obtained (of the Abortox type) [4, 5].

Thus, it seems to be convincingly proven that the genesis of antibodies upon vaccination against brucellosis does not correlate with immunity development. This is at least evidenced by the recent trend of developing weakly agglutinogenic and non agglutinogenic vaccines. The issue of the cellular type of immunity in the brucellosis infection seems to be beyond doubt. The experiments with the *Brucella abortus* RB51 vaccine show the cellular nature of the immunity induced by their vaccine [6]. This vaccine is used for the cattle aged four to eleven months at a dosage of 1 – 3 x 1010, and for the cattle aged 11 months — at a dosage of 1 – 3 x 109. In the experiments, the authors did not find antibodies at various times in 3,250 animals after vaccination using the standard methods, and did not find *brucellae* of the vaccine strain in the milk; therefore, a conclusion was made that this vaccine stimulated the cellular type of immunity. Recently, however, reports have reappeared about the positive role of the humoral immunity against the brucellosis infection. The experiments on the mice that were deficient in terms of the B-cells proved that antibodies played a limiting role in the infections with intracellular parasitism, brucellosis in particular [1, 7].

Understanding this issue is of great practical importance. At the present stage, the choice of the adjuvant is of significant importance in constructing killed vaccines, both corpuscular and from their fragments, including those obtained from purified protective antigens. To date, a significant number of immune stimulating drugs have been developed, and their correct selection allows purposeful stimulation of the immune system of either humoral or cellular type.

The purpose of the research was to study the immunogenic and antigenic properties of agglutinogenic and weakly agglutinogenic vaccines against animal brucellosis. This article presents the materials about studying the anti-brucellosis properties of various components (lymphocytes, neutrophils, plasma, and serum) of the blood of immune and intact animals. The authors hope that the results of this study will make a certain contribution to studying the role of antibodies in brucellosis.

MATERIALS AND METHODS

The research was conducted on the basis of the veterinary center of the Yakutsk Research Institute of Agriculture named after M.G. Safronov during 2014-2018 (the project code of the state task for research: 0821-2018-0003 of 04/15/2014).

For the study, the blood from immune and intact animals (cattle) (immune – 30 heads, intact – 30 heads) was separated into component fractions using the method of gradient centrifugation. At the time of the study, 1.5 months had passed after immunization of adult heifers with the vaccine obtained from the *Brucella abortus* 19 strain [1, 3, 8].

The blood from the heifers was taken into sterile tubes with heparin (25 – 50 U/ml). The density gradients were ficoll and verografin solutions (Preparation of density gradient: solutions of ficoll-400 and verografin are mixed. Using a hydrometer, the density of the resulting solution is measured, which should be 1.077 g/cm. If the density is more than necessary, then solution of ficoll-400 should be added, if it is less than necessary, then solution of verographin is added). The blood diluted to 1:3 with Hanks' solution (a ready-made solution is manufactured by Research and Production Enterprise PanEco, Moscow, comprised of inorganic salts and glucose solved in purified water and sterilized through 0.22 μm pore size filters; the solution contains salts of calcium and magnesium) was placed in layers on the density gradient and centrifuged in a horizontal rotor at 400 g for 30 minutes. After centrifugation, three layers formed in the centrifugal tube: the upper — blood plasma; the middle — the density gradient, and the lower — erythrocytes. At the interface of the blood plasma and the density gradient, the layer of lymphocytes (in the form of a light whitish cloud) was carefully sucked off with a sterile Pasteur pipette and transferred to another tube. The layer of polymorphonuclear leukocytes (in the form of a whitish film) was taken at the interface of the blood plasma and the density gradient, and was also transferred to another tube. The isolated blood cells were washed three times in Hanks' solution by centrifugation at 400 g for 10 minutes and re-suspended in Hanks' solution. Various populations of blood cells, serum, and blood plasma were isolated in strict sterility. Blood serum and plasma were used both in the native and heated forms. The plasma and serum were heated to 60 0C for half an hour for the inhibition of heat-labile bactericidal factors of the blood (lysozyme, the complement system, and M-class immunoglobulins).

A suspension of *brucellae* from the *Brucella abortus* 19 vaccine strain obtained from immune and intact animals had been injected into the tubes with various blood fractions until the final concentration of 1 billion microbial cells was reached. The concentration of *brucellae* in the bacterial mass was determined according to the optical standard of turbidity. The required concentration of microbial cells was obtained by a series of bacterial mass dilutions in sterile saline. For monitoring the concentration of *brucellae*, seeding was made into Petri dishes with meat-peptone glucose-glycerol agar (MPGGA) (five dishes for each sample) from the last and the penultimate dilutions of the culture, followed by counting the number of grown colonies.

IIOAB JOURNAL
ISSN: 0976-3104

The concentration of microbial cells was monitored before incubation, immediately after injecting the suspension of *brucellae* into various blood fractions, and six to eight hours after incubation at 37 ºC.

Devices and equipment used in laboratory diagnosis of brucellosis complied with the Appendix 8 "The order of organization and conduct of laboratory diagnosis of brucellosis for laboratories at the territorial, regional and federal levels" of Methodological instructions MUK 4.2.3010-12.

RESULTS AND DISCUSSION

At the initial stage, the authors made a series of experiments for determining the possibility of the cytolytic effect of specific immunoglobulins on the *brucellae* culture in the absence of cells with killer effect, i.e., for determining the viability of *brucellae* under the effect of immune serum. After mixing the *brucellae* suspension with immune serum with an activity of 640 IU, the mixture was incubated at 37 ºC in a thermostat. The experiments were performed with *brucellae* from both the vaccine (*Brucella abortus* 19) and the virulent (*Brucella abortus* 54) strains. After 24 hours, the resulting agglutinate was sown on solid nutrient media. In the reference tubes, saline was used instead of immune serum. One to three days later, the plentiful growth of *brucellae* (in a lawn) started with no visible difference in the experiment and the reference. No significant differences were noted in the growth of the vaccine and the virulent cultures, either.

The experiments showed that *brucellae* could maintain viability even in the conditions of agglutination with their specific immunoglobulins. However, this technique did not allow to accurately determine the degree of the *brucellae* survival ability. Therefore, an experiment was made with the use of the method that involved seeding *brucellae* into Petri dishes and counting the number of grown colonies.

Table 1 shows the data of determining the bactericidal activity of various blood fractions from the intact animals and the animals immune to brucellosis.

Table 1: The bactericidal activity of various blood fractions from the intact animals and the animals immune to brucellosis

Object type			The number of microbial cells (billion)	
			Before incubation	After incubation
Animal blood samples	intact		0.99 ± 0.005	1.25 ± 0.008*
	vaccinated		0.98 ± 0.008	0.96 ± 0.012
Animal blood serum	intact	native	0.99 ± 0.012	0.79 ± 0.008*
		heated	1.01 ± 0.011	1.95±0.005*
	vaccinated	native	1.0 ± 0.012	1.35 ± 0.011*
		heated	0.98 ± 0.002	1.88 ± 0.008*
Animal blood plasma	intact	native	1.1 ± 0.005	0.99 ± 0.005
		heated	1.0 ± 0.012	1.75 ± 0.008*
	vaccinated	native	1.05 ± 0.008	1.2 ± 0.005*
		heated	0.99 ± 0.005	1.65 ± 0.005*
The population of segmented neutrophils from the animals	intact		1.06 ± 0.012	3.95 ± 0.013*
	vaccinated		0.97 ± 0.008	4.89 ± 0.017*
The population of lymphocytes from animals	intact		1.03 ± 0.005	0.99 ± 0.008
	vaccinated		1.1 ± 0.008	0.5 ± 0.009*

Note: * — statistically veracious difference (P < 0.05)

The Table 1 shows that the greatest bactericidal effect was observed in the population of lymphocytes obtained from the immune animals. The number of microbial cells after incubation decreased by more than half (0.5 ± 0.009 bln.m.c.). In the intact animals, these figures were lower (0.99 ± 0.008 bln.m.c.). That is, the number of *brucellae* remained at almost the initial level, although during such an incubation time, in otherwise favorable conditions, it could well have increased. The blood serum indicators were of interest. For *brucellae*, the bactericidal activity of the blood serum taken from an intact animal was higher (0.79 ± 0.008 bln.m.c.) compared to that of the blood serum taken from an immune one (1.35 ± 0.011 bln.m.c.). The blood serum taken from an immune animal not only did not inhibit the growth and reproduction of *brucellae* but even seemed to stimulate them. In any case, the bactericidal activity indicators of immune serum were approaching similar indicators of heated serum.

The decreased inhibitory ability of positive serum, compared to negative serum, was apparently due to a decrease in the levels of lysozyme and the complement, which occurred in the initial period after

IIOAB JOURNAL
ISSN: 0976-3104

immunization with the live vaccine [5, 9], which, in turn, proved the nonspecific inhibitory ability of immune serum to *brucellae*.

Approximately the same was observed with the blood plasma obtained from intact and immune animals as with serum, but it was less pronounced.

The authors have found interesting the fact that after inactivation of the complement and other heat-labile factors, serum (both negative and positive) generally loses its ability to exert any inhibitory effect on the *brucellae*, which may multiply in it, using serum components as a nutritious substrate. By the way, this property of serum is widely used in making culture media for cultivating many microorganisms, including *brucellae*.

The bactericidal properties of the blood obtained from an immune animal (0.96 ± 0.012), compared to the properties of normal blood (1.25 ± 0.008), were more pronounced. Here, the cooperation of all parts of the immune system was observed. The somewhat lower bactericidal activity of the immune blood, compared to that of the lymphocyte population, in the opinion of the authors, was explained quite simply. With the introduction of a suspension of *brucellae* into an isolated population of lymphocytes, the pathogen encountered powerful cooperation of the cells that had a killer effect and nothing more. When the germ was introduced into the blood, the killer effect competed, and not always successfully, with the growth factors in the form of protein, carbohydrates, vitamins, etc. that were abundant in the blood. In this regard, the properties of the population of polymorphonuclear leukocytes were very obvious. It seemed like the *brucellae* had been introduced into an optimally chosen nutrient substrate. The number of *brucellae* grew four times and more both in the normal (3.95 ± 0.013) and in the immune (4.89 ± 0.017) population of neutrophils. However, the microscopy of smears stained by Romanovsky-Giemza showed that the phagocytosis was pronounced, especially in the immune population of neutrophils. Some neutrophils were so overfilled with *brucellae* that they threatened to rupture the membrane. This happened periodically, judging by some conglomerates of *brucellae* and nuclear material of polymorphonuclear leukocytes without cell membranes scattered in various fields of view. The question of whether the rupture of neutrophil shells occurred due to contamination with *brucellae* or as a result of mechanical damage by polished glass when smears kept open. However, the authors prefer the first brucellosis version of this phenomenon, given the significant increase in the number of *brucellae*.

In the experiment, only blood serum and the plasma could be used in a sufficiently pure form. The situation with the populations of cellular blood fractions was somewhat more complicated. Using the suggested method of blood fractionation, the authors failed to obtain a homogeneous population of the blood cells of both polymorphonuclear and mononuclear leukocytes. In the microscopy of the smears with polymorphonuclear leukocytes, the main part of the cells were segmented neutrophils. Basophils and eosinophils, and in studying several tens of visual fields, individual stab and even young neutrophils were found. The mononuclear fraction was presumably represented by various populations of T- and B-lymphocytes since the used method did not allow dividing them into subpopulations. Under smear microscopy, all cells represented an approximately homogeneous mass with some size variation (large and small lymphocytes). The authors were virtually unable to detect monocytes. Apparently, given the adhesion property, lymphocytes were lost during washing three times by centrifugation.

The obtained *in vitro* results cannot fully reflect the *in vivo* events. Yet, based on the results of the studies and the literature, some conclusions may be drawn. One cannot ignore the fact that the inculcated pathogen usually has tens and probably more antigenic determinants, rather than one. As a result of the biochemical structure heterogeneity, some of them may act as strong antigens (for example, polysaccharide antigens, such as lipopolysaccharides of the gram-negative bacteria), while the other induce less significant antigenic stimulus. All this leads to the fact that in many diseases, in particular, brucellosis, the antibodies complementary to the structural components that are not necessary for the life of the microorganism are detected in the highest titers with the standard diagnostic. Blocking of such antigenic macromolecules by the agglutinating and complement-binding antibodies had little effect on the viability of the pathogen. Therefore, it is said in such cases that there is no correlation between the titer of specific antibodies and the protective effect verified in acute experiments by the method of experimental infestation.

The literature that covers the immunology of brucellosis reports that specific antibodies have an opsonizing effect on the cultures of both immune and not immune macrophages, enhancing to some extent their phagocytic and bactericidal ability *in vitro* [3].

Today, several IgG subclasses are known (IgG1, IgG2, IgG3, IgG4), each being more pronounced in a certain serological reaction. Apparently, according to the old classification, the role of the antibodies that are significant in fighting the brucellosis infection and correlate with the immune system may be attributed to precipitins. This kind of antibodies has been detected with the soluble poly-B-antigen in the reaction of radial immunodiffusion (RRID) [6, 7, 10, 11] for differentiating the infected and vaccinated animals. Today, the immunodiffusion reaction with the O-polysaccharide antigen is officially approved in the Russian Federation.

Thus, the antibodies detected in the diagnosis of brucellosis, with the visible manifestations being the agglutinating and the complement-binding effects, most likely play only the role of witnesses of the

IIOAB JOURNAL
ISSN: 0976-3104

immune system's contact with the antigen. The precipitating antibodies, which exhibit an opsonizing effect and can block epitopes that act as the pathogenicity factor, can play a positive role in brucellosis immunity, being, in essence, the protective antigens. Given the prevailing role of the cellular immunity in brucellosis, evaluating the efficacy of some vaccines using agglutinogenicity only is not justified, and does not show the true state of things [6, 10].

CONCLUSION

Based on the results of the studies, the following conclusions may be drawn. The agglutinating and complement-binding antibodies detected in the diagnosis of brucellosis are not essential for brucellosis immunity and play the role of mainly the "witness" of the immune system's contact with the pathogen. Brucellosis immunity is mainly of the cell type, but some precipitin antibodies show the phenomenon of opsonization and blocking the pathogenicity factor, and play a positive role in forming brucellosis immunity. Veracious assessment of the immunogenicity of agglutinogenic and weakly agglutinogenic vaccines against brucellosis is possible only with the use of the direct infestation method. In conclusion, it should be noted that these studies will be the basis in developing precision diagnostic and vaccines for treating brucellosis in animals, and will make it possible to improve the state of the farms affected by brucellosis.

CONFLICT OF INTEREST

The authors declare no competing interests in relation to the work.

ACKNOWLEDGEMENTS

None.

FINANCIAL DISCLOSURE

None.

REFERENCES

[1] Godfroid J. [2017] Brucellosis in livestock and wildlife: zoonotic diseases without pandemic potential in need of innovative one health approaches. Archives of Public Health, 75(1):34.

[2] Kanouté YB, Gragnon BG, Schindler C, Bonfoh B, Schelling E. [2017] Epidemiology of brucellosis, Q fever and Rift Valley fever at the human and livestock interface in northern Côte d'Ivoire. Acta tropica, 165:66-75.

[3] Vinokurov NV, Sleptsov ES, Stepanov AI, Fedorov VI, Robbek NS, Dayanova GI, Ivanov AA. [2019] Testing the biological properties of the vaccine from strain Brucella abortus 75/79-AB on reindeer. Advances in Animal and Veterinary Sciences, 7(S1):40-44.

[4] Dotsev AV, Kharzinova VR, Romanenko TM, Laishev KA, Soloveva AD, et al. [2018] The admixed history of kola peninsula semi-domestic reindeer population inferred from genome-wide SNP analysis. Journal of Animal Science, 96(S3):137-139.

[5] Fedorov VI, Sleptsov ES, Vinokurov NV, Grigoriev II, Zakharova OI, Maksimova AN. [2018] On Adapting Domestic Even Reindeer to the Mountain-Taiga Zone of the North-East of Russia. Journal of Pharmaceutical Sciences and Research, 10(7):1660-1662.

[6] Fedorov AI, Iskandarov MI, Ignatov PE, Al'bertyan MP, Nestrelyaev SS, Nekrasov AV, Khaitov RM, Petrov RV. [2006] The importance of humoral and cellular immunity in brucellosis. Physiology and pathology of the immune system, 10(8):3–7.

[7] Ignatov PE. [2010] Dialogues about the insidious brucellosis. The All-Russian Research Institute for Experimental Veterinary Medicine, Moscow, 103.

[8] Kulakov YK, Zheludkov MM, Sclyarov OD. [2010] Variable-number tandem repeat markers for identification of Brucella abortus 82 and 75/79-AV. Vaccine, 28(S5):41-45.

[9] Fedorov VI, Stepanov AI, Sleptsov ES, Vinokurov NV, Bochkarev II, Maksimova AN. [2018] Northern Domestic Reindeer Husbandry of the Republic of Sakha (Yakutia): Retrospective Analysis and Development Trends. Journal of Pharmaceutical Sciences and Research, 10(10):2559-2563.

[10] Albertyan MP, Iskandarov MI, Fedorov AI. [2013] The immunobiological properties of the weakly agglutinogenic vaccine against brucellosis in farm animals. Veterinary Medicine and Feeding, 4:20–23.

[11] Hoch AA, Sleptsov ES. [2001] Reindeer brucellosis in Yakutia. Sakhapoligrafizdat, Yakutsk, 203(2):289-94.

ARTICLE

COMPARATIVE STUDIES ON TWO DIPLOID COTTON GENOMES REVEALS FUNCTIONAL DIFFERENCES OF BASIC HELIX-LOOP-HELIX PROTEINS IN ARABIDOPSIS TRICHOME INITIATION

Anh Phu Nam Bui[1*], Thozart Bui[2], Tin Phu Dang Bui[2], Tran Thi Huyen Tran[2]

[1]*Faculty of Biotechnology, Ho Chi Minh city Open University, 35 Ho Hao Hon, Ho Chi Minh city, VIETNAM*

[2]*Department of Biological Sciences, Texas Tech University, Box 43131, USA*

ISSN 0976-3104

ABSTRACT

Background: *The cultivated tetraploid cotton species (AD genomes) was originated from two ancestral diploid species (A- and D-genomes). While the ancestral A-genome species produce spinnable fibers, the D- genome species do not. Cotton fibers are unicellular trichomes originating from seed coat epidermal cells, and currently there is an immense interest in understanding the process of fiber initiation and development. Current knowledge demonstrates that there is a great of deal of resemblance in initiation mechanism between by Arabidopsis trichome and cotton fiber.* ***Aims****: In this study, we performed comparative functional studies between A-genome and D-genome species in cotton by using Arabidopsis trichome initiation as a model.* ***Methodology****: Four cotton genes TTG3, MYB2, DEL61 and DEL65 were amplified from A-genome and D-genome species, and transformed into their homolog trichomeless mutants Arabidopsis ttg1, gl1, and gl3egl3, respectively.* ***Results****: Our data indicated that the transgenic plants expressing TTG3 and MYB2 genes from A-genome and D-genome species complement the ttg1 and gl1 mutants, respectively. We also discovered complete absences of two functional basic helix loop helix (bHLH) proteins (DEL65/DEL61) in D- diploid species and one (DEL65) that is functional in A-genome species, but not from D-genome species. This observation is consistent with the natural phenomenon of spinnable fiber production in A- genome species and absence in D-genome species.* ***Conclusions****: These results suggested that MYB2, TTG3 and DEL65, when expressed in Arabidopsis, regulated the regulatory network genes during the trichome initiation process.*

KEY WORDS
Arabidopsis trichome, MYB2, TTG3, DEL65, DEL61

Received: 2 June 2020
Accepted: 19 June 2020
Published: 10 Sept 2020

***Corresponding Author**
Email:
buiphunamanh@yahoo.com

INTRODUCTION

In position-dependent cell fate determination and pattern formation in *Arabidopsis* trichomes have been well-studied. Trichomes are unicellular single-celled structures emerging and differentiating in the leaf epidermal cells. After cell divisions, these structures subsequently become independent of each other [1]. The mature Arabidopsis leaf trichome consists of a stalk and three to four branches, and its function can vary from trapping herbivorous insects, dispersing seeds, reducing transpiration, to protecting the plants from ultraviolet radiation. The morphogenesis of a trichome is characterized by a series of six phases [2], starting with the introduction of trichome initial followed by subsequent radial expansion and completing with the promotion of completely developing trichome. Other cellular activities connected with the trichome maturation from phase one to phase six include endo-reduplication of the nuclear DNA to an average of 32–64C (the ploidy level of original un-replicated cells is 2C), vacuolization during the transition, and the development of surface papillae during phase one through four, phase four to five, phase five and six, respectively [1].

The initiation of *Arabidopsis* single-celled trichome from leaf epidermal cells presents a useful tool to study the genetic pathways and regulatory signals in cell fate regulation [3, 4]. Genetic and molecular research have elucidated trichome development by a transcriptional and regulatory network controlled by trichome activating and suppressing genes. Over thirty genes have been isolated accounting for diverse aspects in trichome formation including trichome initiation, spacing, size, and morphology. Three groups of proteins have been showed to participate in a trimeric complex to promote trichome initiation, including the WD40 protein TRANSPARENT TESTA GLABRA1 (*TTG1*) [4-8], the R2R3 MYB-related transcription factor GLABRA1 (*GL1*) [9], and the basic helix-loop-helix (bHLH)-like transcription factors GL3 and their functionally redundant ENHANCER OF GL3 (*EGL3*) [10, 11]. Upon the assembly of these proteins, the trichome trimeric complex activates transcription of its direct downstream gene glabrous2 (*GL2*) encoding a homeodomain-leucine zipper protein. *GL2* is documented as the primary target gene of the trichome patterning machinery and is accountable for regulating trichome initiation on *Arabidopsis* leaves [1, 3, 12]. Together with *GL2*, *WRKY* transcription factor *TTG2* and cell cycle gene SIAMESE (*SIM*) are also upregulated. *TTG2* is strongly expressed during trichome patterning and differentiation, while SIM controls endo-replication, a process essential for trichome development.

The GL1-GL3/EGL3-TTG1 complex also upregulates a number of homologous R3 single repeat MYB genes that partially redundantly function as trichome initiation suppressors. These include TRIPTYCHON (*TRY*) [13], CAPRICE (*CPC*), ENHANCER OF TRY AND CPC1 (*ETC1*), *ETC2*, *ETC3* [14], TRICHOMELESS1 (*TCL1*), and *TCL2* [15]. It has been proposed that these repressors render the trimeric complex inactive by the competition with GL1 for binding site with GL3, forming the inert complex R3 MYB INHIBITOR-GL3/EGL3-TTG1. The binding and competition with GL1 differ substantially among these repressors. Binding assays suggest that *TRY* shows the strongest binding affinity, while CPC is the most dominant competitor for binding of GL1 to GL3 [16, 17].

Cotton (*Gossypium* spp.) is regarded as one of the most influential crop plants widely cultivated for textile production. Of fifty-two members in *Gossypium* genus, there are 46 diploids (2n = 2X = 26), five well-

established tetraploids, and one purported tetraploid species (2n = 4X = 52). It has been proposed that diploid cotton species may have originated from a common ancestor that subsequently evolved and diversified into eight monophyletic groups denoted as A–G, and K [18-20]. Approximately 1–2 million years ago, there was a spontaneous and interspecific hybridization event between A and D diploids and subsequent polyploidization that introduced a new allotetraploid (AD) lineage. Two diploid *G. herbaceum* (A1), *G. arboretum* (A2) and two allotetraploid Upland cotton species, *Gossypium hirsutum* L (AD1), and Sealand cotton, *G. barbadense* (AD2), are dominating in more than 70 countries and have had significant influence on global economic development [21, 22] . Interestingly, *G. raimondii* (D5) contributes the D-genome of the allotetraploid cottons, yet it does not confer spinnable fibers production as the A-genome donors do (*G. arboreum, G. herbaceum*) [19].

Cotton fibers are seed trichomes. Since both cotton fiber and *Arabidopsis* trichome are single-celled structures differentiated from the ovule and leaf epidermal cells, respectively, it is suggested that these two species could share analogous mechanisms for mediating cell fate determination in trichomes. Compared with the *Arabidopsis* trichome, the underlying mechanism of cotton fiber initiation formation remains elusive. Most of the recent research on cotton fiber development focus on genomic and transcriptomic profiles during the cell elongation stage and secondary wall biosynthesis stage [23-27]. However, the mechanism controlling these pathways still needs to be elucidated.

Previous reports also characterized the importance of transcription factors in cotton fiber developmental pathways. So far, dozens of cotton genes encoding numerous classes of transcription factors have been characterized and found to be upregulated in developing fiber cells. Additionally, many of these cotton genes exhibited high protein sequence similarities to *Arabidopsis* trichome regulators [4, 28]. Ectopic expression of *GaMYB2* from *G. arboreum*, which is homologous to *AtGL1*, rescues the trichomeless phenotype of the *Arabidopsis* gl1 T-DNA mutant and induces a single trichome from the epidermis of *Arabidopsis* seeds, suggesting that *GaMYB2* is a functional homolog of *GL1* [29-31]. Additionally, homologs of *Arabidopsis GL3*, *TTG1, CPC, TRY* and *GL2* (*GaDEL65*, *GaTTG1*, *GaCPC*, *GaTRY*, and *GaHOX1*, respectively) were also isolated from *G. arboreum* and functionally characterized using the *Arabidopsis* trichome model system [31-33]. The four WD-repeat AtTTG1-like genes *GhTTG1–GhTTG4* from the Dt subgenome of the upland cotton *G. hirsutum* have been identified to be constantly expressed in some tissues, such as ovules and fibers [34].

In this paper, we tested if the cotton genes activate the *Arabidopsis* trimeric complex similarly to the *Arabidopsis* genes in initiating the trichome. Our results indicated that transgenic lines with *MYB2*, *TTG3* and *DEL65* from diploid genomes A and D complemented the trichomeless phenotype of gl1-1, ttg1-1 and gl3-1 egl3-77439, respectively. We also analyzed the gene expression of the downstream targets of the trichome initiation complex in three different trichomeless mutants, ttg1-1, gl1-1 and gl3-1 egl3-77439 and complemented lines with their cotton homologs *TTG3*, *MYB2* and *DEL65*, respectively. Our quantitative PCR showed that in transgenic lines with *MYB2*, *TTG3* and *DEL65*, trichome-positive regulators *GL2*, *TTG2*, *SIM*, and *HDG11* were up-regulated while the regulation of trichome suppressors *TRY*, *TCL1*, *ETC1*, and *CPC* were downregulated with the over-production of trichomes on leaves. These results represented a similar regulatory network in trichome formation in *Arabidopsis* transgenic lines complemented with homologous cotton genes.

MATERIALS AND METHODS

Plant materials and growth conditions

The trichomeles *Arabidopsis* gl3-1 egl3-77439 (Kanamycin resistant) double mutant (CS6516), and two single EMS mutants ttg1-1 (CS89) and gl1-1 (CS1644) were previously described by Esch et al. (2003), Humphries et al. (2005), and Guan et al. (2014), respectively [34-36]. All the seeds were obtained from *Arabidopsis* Biological Resource Center (Ohio State University, Columbus, OH). *Arabidopsis* seeds were surface- sterilized by the vapor-phase sterilization method described by Clough and Bent (1998) [37]. Seeds were transferred into 1.5µl tubes, which were subsequently placed in a desiccator jar. Prior to sealing the desiccator, a beaker containing 250ml bleach and 5ml HCl was positioned in the desiccator. Sterilization was carried out 12 hours in the fume hood. Once seeds were collected, they were plated on Murashige and Skoog (MS) medium containing 0.8% phytogel. After vernalization for 2 days by placing in the dark at 4 °C, seeds were finally transferred to a growth chamber with the following environmental conditions: 22 °C, light intensity of 130-150 Em^{-2s-1}, 16:8h, light: dark photoperiod and relative humidity of 80% as described previously [38]. Seven days after germination, seedlings were transplanted to soil and grown until maturity in the same temperature and light conditions. Antibiotic selections were performed by supplementing the MS medium with Kanamycin ($50mg.ml^{-1}$) or Hygromycin ($50mg.ml^{-1}$) or Basta ($50mg.ml^{-1}$).

Cloning of *DEL65*, *TTG3* and *MYB2*

To prepare the 35S::*DEL65*, 35S::*DEL61* and 35S::*TTG3* genomic constructs from cotton genomes A (A1, A2) and D (D1, D2, D9), the entire genomic DNA regions of *DEL65*, *DEL61* and *TTG3* were amplified by PCR and then cloned in pMDC32 vectors. For cloning *DEL65* and *DEL61*, the forward and reverse primers were engineered with AscI and PacI restriction sites with the following sequences [Table A1]: GaDEL65-F/ GaDEL65-R; GaDEL61-F/ GaDEL61-R. For cloning *TTG3*, the forward and reverse primers were engineered with XhoI and NotI restriction sites with the following sequences: GaTTG3-F/ GaTTG3-R: The PCR products were subsequently inserted into CaMV 35S expression cassette of pMDC32 vectors. The *MYB2* sequence from

A and D cotton diploid species was isolated from cotton genomic DNA by the primer pair of XhoI-GhMYB2-F/ NotI-GhMYB2-R. The amplified products were subsequently ligated into the pBARN vector and sequenced.

Genetic complementation

The pMDC32 and pBARN vectors harboring *DEL61*, *DEL65*, *TTG3* and *MYB2* genes were electroporated into *Agrobacterium tumefaciens* GV3101, respectively. Prior to plant transformation, these constructs were verified by sequencing. *A. tumefaciens*-mediated transformation of *Arabidopsis* plants homozygous for double mutant for gl3-1 egl3-77439, homozygous single mutant for gl1-1 and homozygous single mutant for ttg1-1 were performed by the floral dip method with constructs 35S::*DEL65* or 35S::*DEL61*, 35S:: *MYB2*, and 35S:: *TTG3*, respectively [37]. The transgenic seeds were screened on plates containing both Hygromycin and Cefotaxime for selection. For 35S::*MYB2* construct transformation, the transgenic seeds were screened on plates containing Basta for selection. The resistant seedlings were transplanted to soil and phenotypically analyzed.

Phenotypic analyses and microscopy

Arabidopsis wild type and transgenic leaves were collected at the 15-day rosette stage and examined under an Olympus SZ61 industrial microscope. Images were taken by 5-megapixel digital color camera Olympus UC50 (Japan).

RNA extraction, cDNA synthesis and quantitative PCR

Transgenic plants with trichome recovery phenotype were subjected to RNA extraction. Total RNA from *Arabidopsis* wild type, mutants and transgenic plants were extracted from 100 mg three-week-old leaf tissues using SpectrumTM Plant Total RNA Kit (Sigma-USA) in accordance with the manufacturer's instructions. For synthesis of the first strand cDNA, RNA was treated with RNase-free DNase I (Sigma, USA) to eliminate genomic DNA, and two µg of total DNA-free RNA were used to synthesize first strand cDNA with iScriptTM Reverse Transcription Supermix RT-qPCR (Bio-Rad, USA) in accordance with the manufacturer's instructions.

For Real time quantitative PCR, double-strand cDNA samples were diluted with water to 0.025 to 0.005 times depending on the concentration of the first-strand cDNA samples. Eight downstream target genes- *GL2* (Q186_GL2_F/Q186_GL2_R), *HDG11* (Q204_HDG11_F/Q205_HDG11_R), *SIM* (Q202_SIM_F/Q203_SIM_R), *TTG2* (Q188_TTG2_F/Q189_TTG2_R), *CPC* (Q180_CPC_F/Q181_CPC_R), *ETC1* (Q184_ETC1_F/Q185_ETC1_R), *TCL1* (Q200_TCL1_F/Q201_TCL1_R), and *TRY* (Q182_TCL1_F/Q201_TCL1_R) were amplified. Primers of target gene and control gene ACTIN (Q9At-Actin-F/Q10At-Actin-R) were listed [Table A1]. Quantitative PCR was conducted with FastStart DNA Green Master (Roche-USA) in accordance with the manufacturer's instructions, and a Roche Real-time detection system Light Cycler 96 was used to detect and determine the differential expression of the studied genes. Quantitative PCR data were analyzed by using ΔΔCt method [39].

Table 1: Primer sequences

Primer	Sequence
GaDEL65-F	GCTTGGCGCGCCATGTCTACTGGAGTTCAACATCAAG
GaDEL65-R	GGCCTTAATTAATCAACACTTGCCAGCAATTCTTTGC
GaDEL61-F	ATCGCTCGAGATGGCTACTACCGGGGTTCAAAATCAAG
GaDEL61-R	ATCGGCGGCCGCCTAAAAAGATTGTTTTACCCTTGATTTTATAGTCACAG
GaTTG3-F	GCCGCTCGAGATGGAGAATTCAACTCAAGAATCCCACCTG
GaTTG3-R	ATCGGCGGCCGCTCAAACTTTGAGAAGCTGCAATTTGTTGG
*Xho*I-*GhMYB2*-F	ACTGGCGGCCGCATGGCTCCAAAGAAGGATGGAGT
*Not*I-*GhMYB2*-R	ACTGCTCGAGTTATACCATTGCTAATGGATCC
Q9*At-Actin*-F	GCACCCTGTTCTTCTTACCG
Q10*At-Actin*-R	AACCCTCGTAGATTGGCACA
Q180_*CPC*_F	CAAGGCTTCTTGTTCCGAAG
Q181_*CPC*_R	GCCGTGTTTCATAAGCCAAT
Q182_*TRY*_F	TGTCGGTGATAGGTGGGATT
Q183_*TRY*_R	GACGGTGAGGCTTGGTATGT
Q184_*ETC1*_F	CCAACCATTGTTGCCTCTTC
Q185_*ETC1*_R	TCATCACCCAAAACCTCTCA

Q186_*GL2*_F	CCCCTCTGGATTCTCAATCA
Q187_*GL2*_R	GACGAGGTTTGTCACGGATT
Q188_*TTG2*_F	GAAGCAGGAGTATCGCAAGG
Q189_*TTG2*_R	GATCATCACTCGCTCGTTCA
Q200_*TCL1*_F	AAGAAGAGTGGTGGGACGTG
Q201_*TCL1*_R	TGATGAGGAGAACCCCACTC
Q202_*SIM*_F	CTTTACACGTCGACCCACTC
Q203_*SIM*_R	CATACTTGTGCATGTGCCTCT
Q204_*HDG11*_F	ATATGGAGTCGGTGGAAACG
Q205_*HDG11*_R	GCATTGAAGGCAAAAGAAGG

RESULTS

Complementation studies

Transgenic plants expressing *TTG3* and *MYB2* genes from A and D diploids complemented the ttg1-1 and gl1-1 mutants, respectively. However, ectopic expression of *DEL65* from the A diploid rescued the gl3-1 egl3-77439 mutant, while over expression of *DEL65* from the D- diploid did not recover the double mutant phenotype [Fig. 1]. This observation was consistent with the natural phenomenon of spinnable fiber production in the A- genome species and absence in the D- genome species. Since these results were from one each of these species, we have characterized the *DEL65* from other available A and D diploid species. Genomic DNA of *DEL65* was cloned from A1 (*G. herbaceum*), A2 (*G. arboreum*), D1 (*G. thurberi*), D2 (*G. armourianum*), and D9 (*G. laxum*) species and transformed into the gl3-1 egl3-77439 double mutant. Conclusively, *TTG3* and *MYB2* from both A and D genomes species, and only *DEL65* from A diploid species complemented the trichomeless phenotype.

Fig. 1: From top to bottom: Complementing assays on trichome phenotype were performed on *ttg1-1* single mutant, *gl1-1* single mutant, and *gl3-1 egl3-77439* double with *TTG3*, *MYB2*, and *DEL61*, *DEL65*, respectively. Arrows indicate trichome initiation on first true leaves of transgenic plants.

Since *Arabidopsis* has functionally redundant bHLH proteins (GL3 and EGL3) involved in trichome initiation, the cotton diploids might contain functionally redundant proteins contributing to fiber formation. Genome wide analysis for the presence of DEL65 homolog in A and D diploid was performed and we found the presence of a

IIOAB JOURNAL
ISSN: 0976-3104

closely-related protein, a single copy *DEL61* in both genomes (A-genome: accession number GCA_00642285.2 from position 95853928 bp to position 95856825 bp and D-genome: accession number PRJNA82769 from position 1682788 bp to position 1685967 bp). The *DEL61* was amplified from A and D diploid species independently, and subsequently transformed into gl3-1 egl3-77439 double mutants. Interestingly, the DEL61 from both diploids did not complement the trichomeless phenotype of the double mutant [Fig. 1]. Taken together, our complementing assays illustrated that the lack of spinnable fiber production in the D- diploids could be attributed to the complete absence of functional *DEL65* and *DEL61*. The non-functionality of these two bHLH proteins may not be the only reason to explain why D- genome does not confer spinnable fiber production, but it could be one of the key factors missing in D diploid species.

Conclusively, based on the *Arabidopsis* trichome model system, it demonstrated the functional differences in DEL65 between A and D diploid species. Sequence comparison demonstrated that there is 96.7% homology in *DEL65*-A and *DEL65*-D at DNA level and yet *DEL65*-D is not functional, therefore, it is highly fascinating to investigate the molecular basis for functional differences of DEL65 in future studies.

Gene expression analysis

Trichomes are well patterned on *Arabidopsis* leaves due to the lateral inhibition mechanism [13] while there is no apparent pattern in fiber formation on cotton seed. Our complementing assays illustrated that transgenic lines with *MYB2*, *TTG3* from genome- A and -D, *DEL65* from genome- A rescued the trichomeless phenotype of gl1-1, ttg1-1, gl3-1 egl3-77439, respectively. However, trichome initiation in transgenic lines with one cotton gene in the *Arabidopsis* trimeric complex still reflected defined pattern on *Arabidopsis* leaves [Fig. 1].

In order to answer the question of pattern difference, we conducted quantitative PCR to observe if there is any difference in gene expression of downstream target genes responsible for trichome promoting regulated by trimeric complex in wild type, trichomeless mutants, and transgenic lines from cotton genomes A and D. Eight candidate target genes were chosen from published data [40].

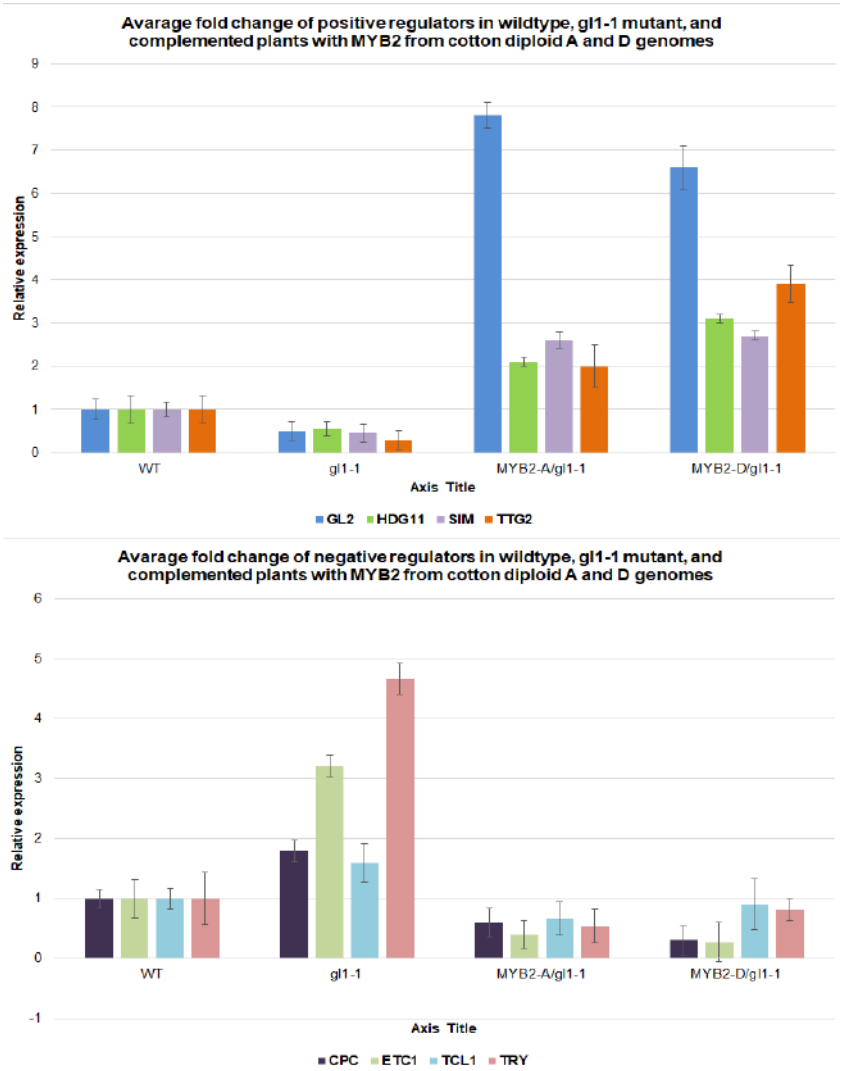

Fig. 2: Transcript levels for individual gene copies of the four trichome negative genes and four positive regulatory genes in Arabidopsis wild type, gl1-1, 35S::*MYB2*-A/ gl1-1 and 35S::*MYB2*-A/ gl1-1

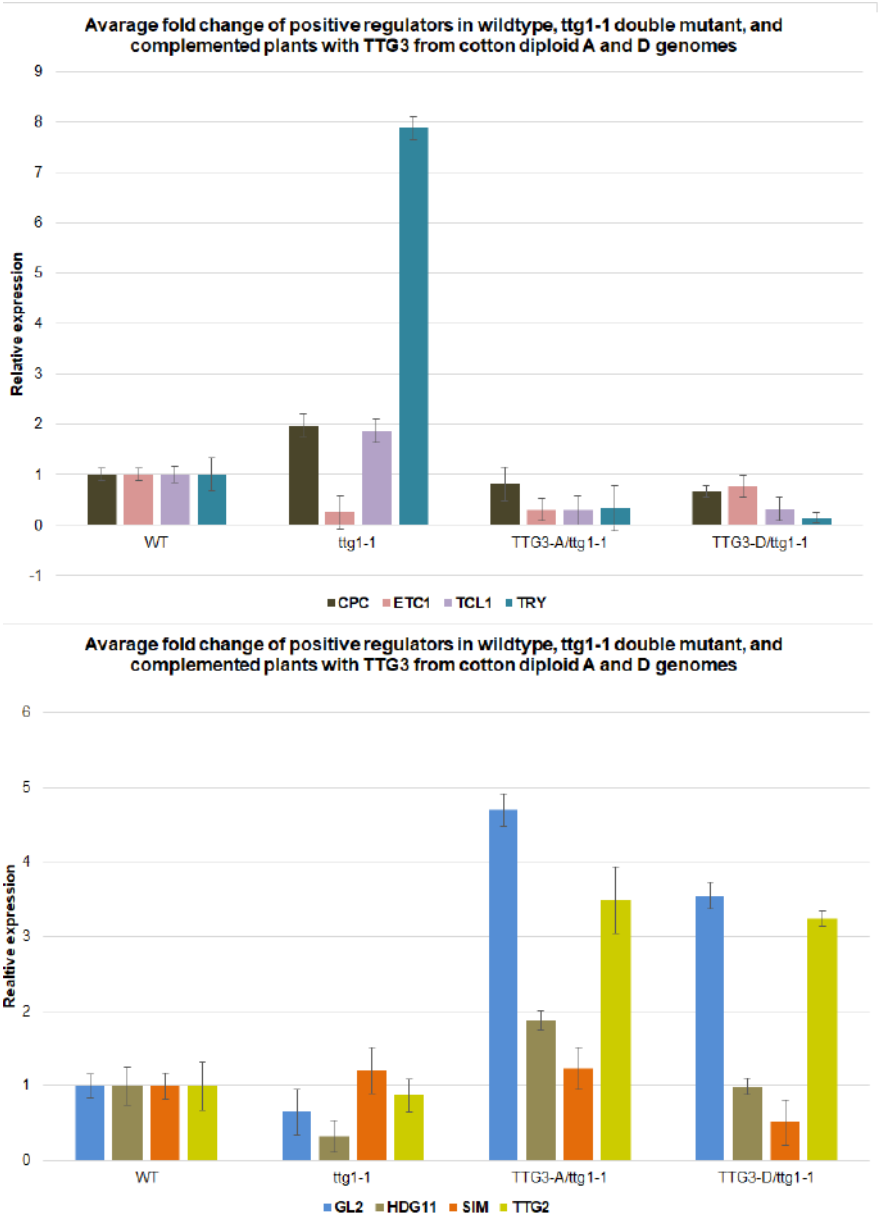

Fig. 3: Transcript levels for individual gene copies of the four trichome negative regulatory genes and four positive regulatory genes in *Arabidopsis* wild type, double mutant ttg1-1, 35S::*TTG3*-A/ ttg1-1 and 35S::*TTG3*-D/ ttg1-1

Figure 2 shows differential expression of four positive and four negative regulators in *Arabidopsis* leaves trichome initiation in wild type, glabrous mutant gl1- 1 and its respective transgenic lines complemented from diploid A and D cotton genomes. The expression of four positive regulators were significantly elevated in transgenic *GaMYB2/* gl1-1 and *GrMYB2*/gl1-1, which could be attributed to the trichome initiation phenotype compared to the mutant gl1-1. It has been documented that *GL2* is required for *Arabidopsis* trichome initiation of leaves while *TTG2* is predominantly up-regulated in trichomes throughout their development. Two other positive regulators, i.e. *HDG11* and *SIM* are responsible for normal trichome branching and development, respectively. The down-regulated expression of R3 *MYB* repressor genes, namely CPC, ETC1, *TCL1* and *TRY*, was consistent with the over production of trichomes on leaves of 35S:: *MYB2*-A/gl1-1 and 35S:: *MYB2*-D/gl1-1 compared to gl1-1. Similar regulation was observed in eight target genes stimulated by trimeric complex in transgenic plants with *TTG3* from cotton diploids A and D genomes compared with wild type and ttg1-1 mutant [Fig. 3].

The regulation of downstream target genes in transgenic lines gl3-1 egl3-77439 transformed with *DEL65* from cotton A- and D- genome species further confirmed the consistency from our complementing assays [Fig. 4]. The transcript levels of positive trichome regulators including *GL2*, *TTG2*, *HDG11*, and SIM were increased, and trichome suppressors such as *TRY*, *ETC1* and *TCL1* were and decreased in 35S:: *DEL65*-A/gl3-1 egl3-77439 line than in 35S:: *DEL65*-D/gl3-1 egl3-77439. Surprisingly, we noticed a significant increase (at least three fold) in one R3 *MYB* transcripts, CPC in 35S:: *DEL65*-A/gl3-1 egl3-77439 line, which were not in

agreement with leaf trichome phenotype [Fig. 4]. We speculated that the increasing level of CPC functioning as a counteract or to suppress the exceedingly high elevation of *DEL65* transgene, thus developing an equilibrium feedback control to prevent supernumerary trichomes.

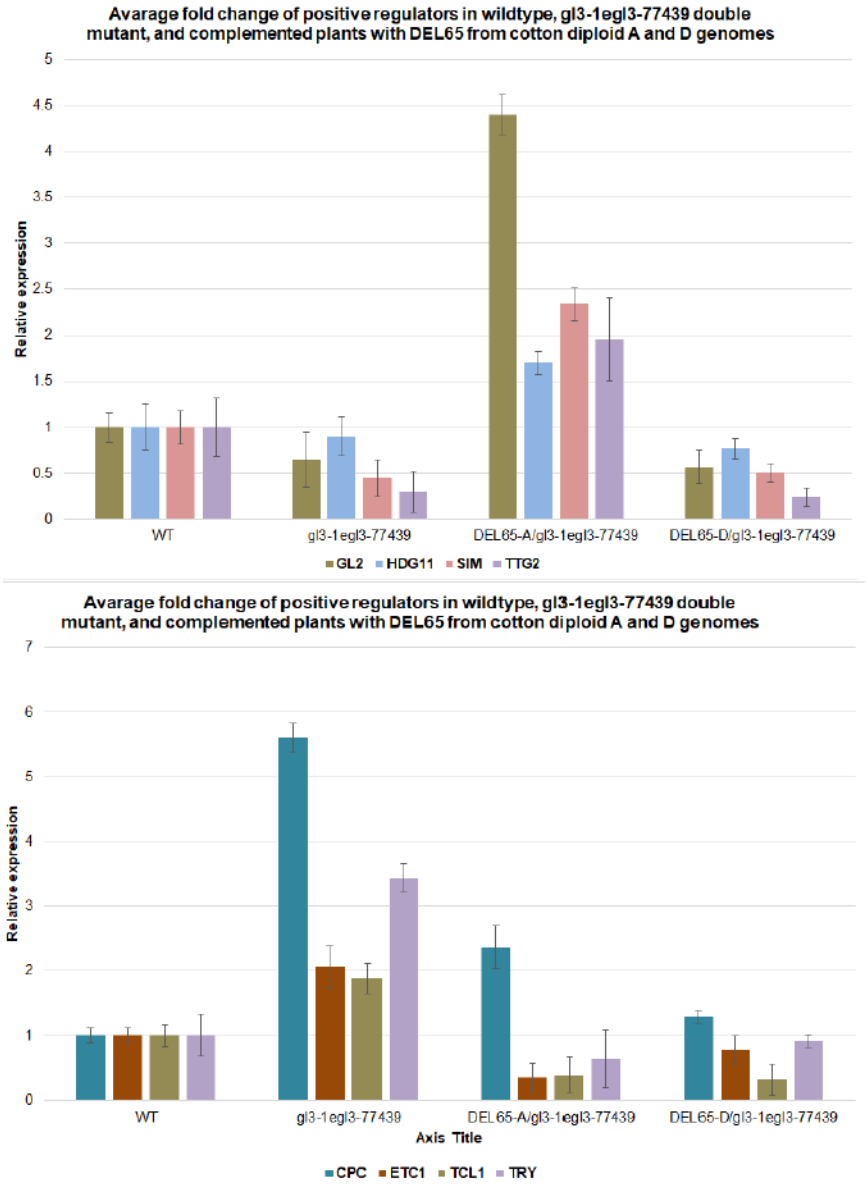

Fig. 4: Transcript levels for individual gene copies of the four trichome negative regulatory genes and four positive regulatory genes in *Arabidopsis* wild type, gl3-1 egl3-77439, 35S::*DEL65*-A/ gl3-1 egl3-77439 and 35S::*DEL65*-D/ gl3-1 egl3-77439

DISCUSSION

In *Arabidopsis*, previous genetic analysis has revealed that trichome initiation is positively mediated by a trimeric activation complex comprised of GL1, GL3 which acts redundantly with its close homolog *EGL3*, and *TTG1* [41, 42]. We studied the functionality of four individual cotton genes *MYB2*, *TTG3*, *DEL65* and *DEL61* from diploid cotton A and D genomes, which show high similarity in sequence with *GL1*, *TTG1*, *GL3* and *EGL3*, respectively, in their respective *Arabidopsis* glabrous mutants. Our complementation assays proved that transgenic lines with *MYB2*, *TTG3* from diploid genomes A and D could rescue the trichomeless phenotype of gl1-1 and ttg1-1 respectively; however, *DEL61* from both the species could not rescue this phenotype of gl3-1 egl3-77439 double mutant. Interestingly, the *DEL65* from A- species rescued the gl3-1 egl3-77439 double mutant but not from D- diploid species. Comparative quantitative PCR analysis of the downstream regulatory network genes showed a similar pattern for *MYB2*, *TTG3* complemented lines from A- and D- diploid species. Comparative analysis of the *DEL65* from A- (rescued the trichomeless phenotype) and D- (did not rescued the trichomeless phenotype) showed differential expression of regulatory network genes between these two lines. These results showed that the cotton genes, when expressed in *Arabidopsis*, regulate the regulatory network genes during the trichome initiation process.

IIOAB JOURNAL
ISSN: 0976-3104

CONCLUSION

In this paper, we employed the *Arabidopsis* trichome model system to examine the mechanism of spinnable fiber production trait. The core trichome initiation complex consisting of bHLH, WD40 and R2R3-MYB proteins was tested for functional differences between A and D genomes, the parental species of the cultivated tetraploid species. The only discrepancy in our complement assays was DEL65 from A- genome species, not D- genome species, complemented the gl3-1 egl3-77439 trichomeless phenotype, reflecting the consistency of the observation that spinnable fiber production trait is absent in D-diploid species. We also tested the regulation of eight target genes stimulated by the trimeric complex in six different transgenic lines transformed with three cotton genes. The expression of trichome positive regulator was significantly elevated which could be attributed to the trichome initiation phenotype, whereas the transcripts level of trichome suppressors were down regulated. However, CPC levels in 35S:: *DEL65*-A/gl3-1 egl3-77439 line were increased, possibly demonstrating a feedback loop to avoid extreme number of trichome initiation. Conclusively, by implementing trichome initiation in *Arabidopsis* as a model, this study provided functional characterization of four cotton important genes from two diploid cotton genomes -A and -D in fiber initiation. However, more studies should be conducted in other diploid cotton genomes to elucidate the understanding the mechanism of fiber initiation mechanism in cotton.

CONFLICT OF INTEREST

There is no conflict of interest

ACKNOWLEDGEMENTS

We would like to thank Dr. Venu Mendu and Dr. Ning Yuan for their valuable advices for our experiments.

FINANCIAL DISCLOSURE

None.

REFERENCES

[1] Hulskamp M. [2004] Plant trichomes: a model for cell differentiation. Nat Rev Mol Cell Biol, 2004. 5(6):471-480.
[2] Szymanski DB, Jilk RA, Pollock SM, Marks MD. [1998] Control of GL2 expression in Arabidopsis leaves and trichomes. Development, 125(7):1161-1171.
[3] Larkin JC, Brown ML, Schiefelbein J. [2003] How do cells know what they want to be when they grow up? Lessons from epidermal patterning in Arabidopsis. Annual Review of Plant Biology, 54(1):403-430.
[4] Serna L, Martin C. [2006] Trichomes: different regulatory networks lead to convergent structures. Trends in Plant Science, 11(6):274-280.
[5] Walker AR, Davison PA, Bolognesi-Winfield AC, James CM, Srinivasan N, Blundell TL, Esch JJ, Marks MD, Gray JC. [1999] The TRANSPARENT TESTA GLABRA1 locus, which regulates trichome differentiation and anthocyanin biosynthesis in Arabidopsis, encodes a WD40 repeat protein. The Plant Cell, 11(7):1337-1350.
[6] Glover BJ. [2000] Differentiation in plant epidermal cells. Journal of Experimental Botany, 51(344):497-505.
[7] Schiefelbein J. [2003] Cell-fate specification in the epidermis: a common patterning mechanism in the root and shoot. Current Opinion in Plant Biology, 6(1):74-78.
[8] Ramsay NA, Glover BJ. [2005] MYB–bHLH–WD40 protein complex and the evolution of cellular diversity. Trends in Plant Science, 10(2):63-70.
[9] Oppenheimer DG, Herman PL, Sivakumaran S, Esch J, Marks MD. [1991] A myb gene required for leaf trichome differentiation in Arabidopsis is expressed in stipules. Cell, 67(3):483-493.
[10] Payne CT, Zhang F, Lloyd AM. [2000] GL3 Encodes a bHLH Protein That Regulates Trichome Development in Arabidopsis Through Interaction With GL1 and TTG1. Genetics, 156(3):1349-1362.
[11] Zhang F, Gonzalez A, Zhao M, Payne CT, Lloyd A. [2003] A network of redundant bHLH proteins functions in all TTG1-dependent pathways of Arabidopsis. Development, 130(20): 4859-4869.
[12] Serna L. [2004] A Network of Interacting Factors Triggering Different Cell Fates. The Plant Cell, 16(9):2258-2263.
[13] Schellmann S, Schnittger A, Kirik V, Wada T, et al. [2002] TRIPTYCHON and CAPRICE mediate lateral inhibition during trichome and root hair patterning in Arabidopsis. The EMBO Journal, 21(19):5036-5046.
[14] Tominaga R, Iwata M, Sano R, et al. [2008] Arabidopsis CAPRICE-LIKE MYB 3 (CPL3) controls endoreduplication and flowering development in addition to trichome and root hair formation. Development, 135(7):1335-1345.
[15] Wang S, Kwak SH, Zeng Q, et al. [2007] TRICHOMELESS1 regulates trichome patterning by suppressing GLABRA1 in Arabidopsis. Development, 134(21):3873-3882.
[16] Wang S, Hubbard L, Chang Y, et al. [2008] Comprehensive analysis of single-repeat R3 MYB proteins in epidermal cell patterning and their transcriptional regulation in Arabidopsis. BMC plant biology, 8:81-81.
[17] Wester K, Digiuni S, Geier F, et al. [2009] Functional diversity of R3 single-repeat genes in trichome development. Development, 136(9):1487-1496.
[18] Fryxell PA, Craven LA, Stewart JM, et al. [1992] A Revision of Gossypium Sect. Grandicalyx (Malvaceae), Including the Description of Six New Species. Systematic Botany, 17(1):91-114.
[19] Wendel JF, Cronn RC. [2003] Polyploidy and the evolutionary history of cotton, in Advances in Agronomy, Academic Press, 139-186.
[20] Wendel JF, Flagel LE, Adams KL, et al. [2012] Jeans, Genes, and Genomes: Cotton as a Model for Studying Polyploidy, in Polyploidy and Genome Evolution, SP Soltis ED Soltis, Editors. Springer Berlin Heidelberg: Berlin, Heidelberg, 181-207.
[21] Zhang BH, Feng R. [2000] Cotton resistance to insect and pest-resistant cotton. Beijing: Chinese Agricultural Science and Technology Press. https://doi.org/10.1073/pnas.1721436115.
[22] Stephens SG, Moseley ME. [1974] Early Domesticated Cottons from Archaeological Sites in Central Coastal Peru. American Antiquity, 39(1):109-122.
[23] Arpat A, Waugh M, Sullivan J, et al. [2004] Functional genomics of cell elongation in developing cotton fibers. Plant Molecular Biology, 54(6):911-929.
[24] Shi YH, Zhu SW, Mao XZ, et al. [2006] Transcriptome Profiling, Molecular Biological, and Physiological Studies Reveal a Major Role for Ethylene in Cotton Fiber Cell Elongation. The Plant Cell, 18(3):651-664.
[25] Udall JA, Swanson JM, Haller K, et al. [2006] A global assembly of cotton ESTs. Genome Research, 16(3):441-450.
[26] Wu Y, Machado AC, White RG, et al. [2006] Expression Profiling Identifies Genes Expressed Early During Lint Fibre Initiation in Cotton. Plant and Cell Physiology, 47(1):107-127.

[27] Samuel YS, Cheung F, Lee JJ, et al. [2006] Accumulation of genome-specific transcripts, transcription factors and phytohormonal regulators during early stages of fiber cell development in allotetraploid cotton. The Plant Journal, 47(5):761-775.
[28] Guan X, Yu N, Shangguan X, et al. [2007] Arabidopsis trichome research sheds light on cotton fiber development mechanisms. Chinese Science Bulletin, 52(13):1734-1741.
[29] Wang S, Wang JW, Yu N, et al. [2004] Control of Plant Trichome Development by a Cotton Fiber MYB Gene. The Plant Cell, 16(9):2323-2334.
[30] Guan X, Lee JJ, Shi X, et al. [2011] Activation of Arabidopsis Seed Hair Development by Cotton Fiber-Related Genes. PLoS ONE, 6(7): e21301.
[31] Guan X, Song Q, Chen ZJ, et al. [2014] Polyploidy and small RNA regulation of cotton fiber development. Trends in Plant Science, 19(8):516-528.
[32] Wang G, Zhao GH, Jia YH, et al. [2013] Identification and Characterization of Cotton Genes Involved in Fuzz-Fiber Development. Journal of Integrative Plant Biology, 55(7):619-630.
[33] Guan XY, Li QJ, Shan CM, et al. [2008] The HD-Zip IV gene GaHOX1 from cotton is a functional homologue of the Arabidopsis GLABRA2. Physiologia Plantarum, 134(1):174-182.
[34] Humphries J, Walker A, Timmis J, et al. [2005] Two WD-repeat genes from cotton are functional homologues of the Arabidopsis thaliana TRANSPARENT TESTA GLABRA1 (TTG1) gene. Plant Molecular Biology, 57(1):67-81.
[35] Esch JJ, Chen M, Sanders M, et al. [2003] A contradictory GLABRA3 allele helps define gene interactions controlling trichome development in Arabidopsis. Development, 130(24):5885-5894.
[36] Guan X, Nah G, Shi X, et al. [2014] miR828 and miR858 regulate homologous MYB2 gene functions in Arabidopsis trichome and cotton fibre development, 5: 30-50.
[37] Clough SJ, Bent AF. [1998] Floral dip: a simplified method for Agrobacterium-mediated transformation of Arabidopsis thaliana. The Plant Journal, 16(6):735-743.
[38] Junker A, Muraya MM, Weigelt-Fischer K, et al. [2015] Optimizing experimental procedures for quantitative evaluation of crop plant performance in high throughput phenotyping systems. Frontiers in plant science, 5:770-770.
[39] Yuan J, Yue H, Zhang M, et al. [2016] Transcriptional profiling analysis and functional prediction of long noncoding RNAs in cancer. Oncotarget, 7(7):8131-8142.
[40] Morohashi K, Grotewold E. [2009] A Systems Approach Reveals Regulatory Circuitry for Arabidopsis Trichome Initiation by the GL3 and GL1 Selectors. PLoS Genet, 5(2):e1000396.
[41] Wang Z, Yang Z, Li F. [2019] Updates on molecular mechanisms in the development of branched trichrome in Arabidopsis and non-branched in cotton. Plant biotechnology journal, 17(9):1706-1722.
[42] Sato Y, Shimizu-Inatsugi R, Yamazaki M, et al. [2019] Plant trichomes and a single gene GLABRA1 contribute to insect community composition on field-grown Arabidopsis thaliana. BMC Plant Biology, 19(1):163.

ARTICLE

OVERVIEW OF ROUGHAGE FEEDS PROCUREMENT TECHNOLOGY

I.Y. Tyurin[1]*, G.V. Levchenko[1], S.A. Makarov[1], Y.V. Komarov[1], I.V. Ryzhkova[2], Y.A. Dugin[3]

[1]Faculty of Engineering and Environmental Management, Saratov State Agrarian University named after N. I. Vavilov, Teatralnaya Square, 1, Saratov, 410012, RUSSIA

[2]Faculty of Economics and Management, Saratov State Agrarian University named after N. I. Vavilov, Teatralnaya Square, 1, Saratov, 410012, RUSSIA

[3]Faculty of Engineering and Technology, Volgograd State Agrarian University, Universitetskiy Avenue, 26, Volgograd, 400002, RUSSIA

ISSN 0976-3104

ABSTRACT

A study of the drying process by means of active ventilation carried out by the authors allows concluding that the patterns of water-yielding capacity in cut plants and changes in the quality of the dried mass at individual stages of drying depend on the properties of the plants themselves and the methods of drying. Knowing these patterns allows choosing the best drying conditions, as well as technological tools for various climatic conditions and various types of crops. The criterion for the process of removing moisture from the dried material by means of active ventilation includes obtaining high-quality conditioned feed at the maximum performance of the equipment while maintaining its nutritional value. When drying with heated air or with gas-air mixture, thermal and moisture conductivity provides additional resistance to moisture movement. To eliminate this resistance, it is necessary to apply low temperatures and an increased speed of the drying agent at the beginning of drying; this ensures faster and more uniform heating of the product. Modern drying methods are characterized by intensification of heat and mass transfer processes, which is achieved in various ways: by increasing the contact surface between the dried product and the drying agent; decrease in relative humidity of the drying agent; the use of combined heat supply; increasing the speed of movement of the dried material and drying agent; a combination of dehydration with various technological processes, etc. Therefore, taking into account the influence of all the objective laws, during research, special attention should be paid to the improvement of the technology and necessary equipment for procurement of roughage feeds using cheap sources. In connection with the foregoing, the task was to study the uniformity of the distribution of the air agent through the air distribution channel to stabilize the forces of aerodynamic resistance to air flow that arose in the dried mass when using infrared burners as thermal energy, which made it possible to substantiate the design of the dryer and optimize the design and technological parameters of the drying.

KEY WORDS
humidity, moisture exchange, drying, herbs, dehydration

Received: 4 May 2020
Accepted: 17 Sept 2020
Published: 26 Sept 2020

***Corresponding Author**
Email:
igor.yu.tyurin@mail.ru

INTRODUCTION

In modern conditions, the main task of agricultural producers should be the procurement of high-quality feed containing maximum nutrients used by the body of the animal to produce meat, fat, milk, etc. [1-9]. Currently, the need for animal feed is not fully satisfied. Production of feed per one conditional head of cattle had been 21.5 - 23.5 cwt of feed units per year during the last twenty years, which was significantly lower than the normative indicator (35-40 cwt of feed units), and their consumption during this period was 71-80% of the norm. Therefore, special attention should be paid to the intensification of feed production [2, 4, 5, 7, 10]. However, at present not all farms have the necessary equipment and technologies [5-14], therefore, it is necessary to prepare appropriately the feed maintaining high level of vitamins. As a consequence, the cost of feed production per unit of the final product is increased by 1.5–2 or more times, as well as the cost of feed itself [5-9]. From studies carried out at different times [1-9], we know that vitamins play the role of unique biological catalysts in animals.

The experience of livestock breeders in Holland, Switzerland, and other countries shows that grazing of dairy cows on grass is the cheapest method of producing milk. Farmers and researchers invest large amounts of money in the improvement of technologies for production and cultivation of crops [5-9]. Costs pay off with interest. Some farmers obtain even more milk in the winter than in the summer by feeding their livestock with roughage. Concentrates are used sparingly, especially since grain prices are quite high. The most used are green grass, haylage, silage, and hay obtained from cultivated land. In other words, today, it is possible to increase the production of milk and meat at least by a factor of 1.5, if a natural forage field is used. The potential of Russian meadows is very high. Russian lands are able to feed herds in the summer and significantly replenish feed supplies for the winter, but their rich potential is poorly used. [5-9].

Therefore, the research was aimed at increasing the quality of feed preparation by improving the technological process and technical means of their drying in the farm [5-7, 9, 12, 13].

ORGANIZATION OF THE TECHNOLOGICAL PROCESS OF FEED PREPARATION

Factors influencing the feed preparation technology

Haymaking at farms of various forms of ownership takes place in various climatic conditions, which affects both the amount of hay harvested and its quality. It should be remembered that high-quality hay is

IIOAB JOURNAL
ISSN: 0976-3104

especially necessary for highly productive animals – dairy cows, beef cattle, etc. Therefore, in order for the productive potential of animals to be high, it is necessary to properly organize the technological process of the roughage procurement.

The complexity of solving the problem arising from the variety of factors causing losses during hay harvesting still does not allow developing a unified methodology for their accounting and applying it to determine the most accurate quantitative indicators under various conditions and methods of roughage procurement. Most researchers who analyze the causes of nutrient loss in procured feeds agree that the most valuable parts of plants are leaves, inflorescences, and the thin parts of stems that are of great nutritional value. However, they dry faster than the bulk of the stems and, unfortunately, when tedding, raking, and other manipulations with the hay during the harvesting process, they easily crumble and are permanently lost. Leaves contain 2-3 times more protein than stems [5, 8]. According to Shain and Borinevich, the leaves of various types of legumes contain 23.4-31.4% of protein, while the stems contain 9.05-11.2% [5, 8]. These parameters are lower for grasses and amount to 4-8%. If the plant mass is exposed to rain during harvesting the losses might increase sharply.

In the course of improving the drying methods, it turned out that moisture removal during drying takes place only in certain drying regime conditions, such as the rate of the air supply, the moisture absorption capacity of the air, and the loss of air pressure in the hay layer. Therefore, to obtain hay with high nutrient content, it is necessary to study the interrelation between the main structural and operational parameters of the equipment used for the procurement [5-9].

Therefore, in modern conditions, the technology should be as cost-effective as possible and contribute to the reduction of the costs per unit of the final product [5-9]. At the same time, the improvement of the existing technologies should ensure their cost-effectiveness.

Mechanical drying

An analysis of the studies shows that a decrease in the moisture content of the object being dried can be achieved in different ways. In the case of expression (mechanical method), the slightly expressed plant mass is laid out for 3-4 hours in a thin layer, which is constantly tedded and then stored. However, this method has a drawback. Nutrients are removed from the mass being dried along with the moisture. Absorption is a contact method, which uses a moisture-absorbing substance. The mass being dried is interlayered or mixed with any other (dry) moisture-absorbing substance. However, in this case, the quality of the procured product decreases.

Chemical dehydration

According to the literature, the chemical method of dehydration was tested with regard to the crop being procured, both directly at the grassroots and after cutting or harvesting. Published research data showed that no promising results were obtained.
This method involves the use of various chemicals. Their use does not lead to direct drying of the material, these substances only act as antiseptics that prevent the development of mold on the mass being dried.

Thermal drying

The most widely used method is thermal drying – thermal removal of moisture. It is simple and affordable for drying of various capillary-porous colloidal objects. Moisture, in this case, is removed in various ways. It can be done directly in the field by air drying and subsequent final drying at the farm using active ventilation. It can be done at the farm by using kiln-drying or final drying with the use of high temperature, using intensive drying with heated gas or other drying agents, using heat treatment of material by high-frequency currents or infrared rays, and by gas dehydration by cooling it below the dew point temperature.

The water-yielding capacity of a material, the quality of the resulting product, and its ability to maintain all its properties at different periods of drying and during further storage depends on the drying methods used [5, 8].

Analysis of these methods allows us to conclude that the drying of crops is subject to a number of requirements arising from the requirements for the finished product.

If we know technological features of the drying process, we can trace and investigate the patterns of moisture return in cut plants and changes in the quality of the dried mass at various drying stages with regard to the properties of the plants. This, in turn, will allow choosing the necessary dryer design, the best drying mode, as well as technological tools in various climatic conditions and for various types of crops.

An essential condition for high-quality hay production with the use of forced ventilation is the uniform passage of the drying agent through the layer of dried hay.

Therewith, it is reasonable to use enclosing structures (ground and subsurface trenches, etc.). This way the influence of wind can be eliminated. However, this causes a new problem of uneven airflow across the width and length of hay piled on the air channel [5, 8].

IIOAB JOURNAL
ISSN: 0976-3104

Therefore, the experimental research methodology was as follows:
1. Obtaining experimental values for choosing the optimal power of the emitter and fan, depending on the thickness of the dried layer.
2. Determining the uneven temperature distribution of the drying agent on the surface of the grating depending on the different power of the IR emitters.
3. Determination of the optimal design of the device for the drying of crop products.
In accordance with the goals and methods of experimental studies, it was planned to conduct experiments in three stages: a laboratory experiment, a laboratory field and field (production) experiment.

QUALITY OF FEED PREPARATION DUE TO IMPROVEMENT OF THE TECHNOLOGICAL PROCESS

Theoretical substantiation of the possibility of improving the feed preparation quality

The mechanics of gases is the science of the laws of motion and equilibrium of gases. When transferring heat from combustion products to the objects being heated (when airflow heaters are used), it is necessary to take into account a large number of different factors, including the nature of the movement of combustion products. Therefore, one of the conditions for the effective operation of the drying assembly is the rational organization of the movement of gases. Knowing the laws of gas mechanics, it is possible to determine the resistance created by moving gases in the dryers, air distribution channels, etc. The fans are selected based on these calculations [5-9].

The laws of fluid motion help to study the movement of the gases in the dryer. The volume of liquid, in this case, in contrast to the volume of gas, is practically independent of temperature and pressure. The variation of gas motion (which obeys the laws of fluid motion) is low if the pressure and temperature of the moving gas are constant. The nature of the movement of the jets leaving the nozzles, burners, or air distribution ducts is determined by the nature of the movement of gases in the working space of the dryers (which operate on gaseous and liquid fuels), as well as air heated in electric heaters. Therefore, the main properties of the jets depend on the proper organization of the movement of gases or a drying agent in the dryers.

In other words, the movement that occurs due to the dynamic action of the jets is called streamline motion. Therefore, the movement of the drying agent inside the assembly is organized based on the properties of free and confined jets with regard to the requirements for the thermal operation of dryers.

However, the movement of gases in the working space of the dryers can be characterized as a channeled motion. In this case, the movement is made possible due to the potential energy of the flow. The movement of gases in the air distribution duct occurs in the horizontal channel due to a decrease in static pressure or due to a decrease in geometric pressure.

During the drying process, the drying zone constantly moves as the flow of the drying agent passes through the layer being dried. The speed, at which this zone moves, determines the kinetics of the drying process. Provided that there is equilibrium below and above the drying zone, the kinetics of the process are constant and can be determined by the amount of supplied air per unit of time (usually m3/h). The forces of aerodynamic resistance to airflow that occur in the dried mass due to the fact that it is porous and a certain laminar and turbulent airflow around a porous barrier is present can be calculated using the following formula [5, 8]:

$$Faero = Slam \times V + Cturb \times V2$$

where V is the air velocity (m/s) and Slam and Sturb are the aerodynamic coefficients for laminar and turbulent airflow, respectively.

Therefore, it is impossible to completely remove moisture from the mass being dried under normal drying conditions using the method of active ventilation. In addition, the residual humidity of the capillary-porous object depends on the humidity of the supplied drying agent (j). That is, if the theoretical drying agent humidity is $j = 0$, then the residual moisture content of the capillary-porous object will be $W = 0$, accordingly. However, in actual practice, $j>0$ and; therefore, $W>0$. Accordingly, the moisture value of the supplied drying agent should correspond to a very specific value of the residual moisture of hay in equilibrium. This moisture content of the plant mass is called equilibrium moisture content [5, 8].

The effect of fan power on high-speed air flow

Before starting experimental studies of the temperature distribution of the drying agent on the surface of the grating, it is necessary to find out the optimal speed regime. Acceleration of drying the sunflower is necessary as the higher the flow rate is, the faster the drying process is. However, it should be taken into account that the speed of air passing through the grating must be certain in order to prevent the drying of the sunflower lower layer out. Optimization of the air flow rate is achieved, as a rule, by regulating the fan motor power. By changing the power at any time, it is possible to achieve the optimal flow distribution rate

IIOAB JOURNAL
ISSN: 0976-3104

on the surface of the grating. For this, experiments were carried out in a laboratory setup. Based on the obtained experimental data, dependencies were constructed.

Temperature distribution depending on the IR emitter power

Before starting experimental studies of the uniformity of the air temperature distribution on the surface of the grating, it is necessary to find out the influence of the IR emitter power, at which the heating of the air flow will be most optimal for seed sunflower drying, that is, the temperature of the air flow should not be more than 4000C. Therefore, experiments with IR emitters with different powers were carried out in a laboratory setup. As a result, emitters with the power of 1.5 kW, 2.3 kW and 3.6 kW were selected. The optimum air flow rate was set at 7.6 m/s and remained constant with each emitter of a certain power. On the basis of processed experimental data, the dependences of the uniformity of the temperature distribution on the emitter power were built.

PRACTICE AND PROSPECTS FOR IMPROVING AIR DISTRIBUTION SYSTEMS

Scientific studies in the field of improving air distribution systems, as well as the use of infrared radiation, were developed in the mid-forties and fifties of the last century [5-7, 9, 12, 13]. In addition, many researchers were engaged in improving the technology and technical means for drying [1, 3, 15-29]. The result of these studies was the creation of industrial plants for the heat treatment of bulk materials. Nowadays, various air distribution installations are produced by a number of companies, in particular, SOF Tech Service LLC (Moscow), OPKTB SibNIPTIZh (Novosibirsk region), Start LLC (Moscow region), Russian Food Corporation (Leningrad region), and even by artisan workshops. The infrared drying technology is actively developed by the following companies: in Ukraine - NPK BND LLC (Dnepropetrovsk), SPKB MeNas (Kiev); in Kazakhstan - Vibromash LLP (Ust-Kamenogorsk); in Uzbekistan - Keramika Syntez LLC (Tashkent); in Belarus –VAEM LLC (Minsk). By analyzing abstract publications and Internet data [10, 30-33], it can be concluded that there are few studies in the field of improving air distribution systems, as well as the use of infrared heating when drying feed. In any technological operation associated with the heating of the product, as a rule, all types of heat transfer (conductive, convective, and radiation) take place [5, 7]. In this case, the fraction of radiant heat transfer increases with temperature. An analysis of existing studies shows interest in this component and is present in many works [16, 21, 23, 28]. The use of distributors of the drying agent inside the installation and heat treatment of the dried material, including with IR energy supply, allows identifying promising areas for improving equipment and technology of drying aimed at maximizing the preservation of the original consumer or technological properties of the product.

These data are necessary to correctly apply the well-known I-d diagram in the calculations of the adiabatic drying process of plant material using active ventilation [5, 8].

CONCLUSION

According to numerous studies in various countries, during the development of new systems for the drying of agricultural products using active ventilation, it is essential to reduce dynamic pressure and increase static pressure. This can be achieved by reducing the speed of the drying agent in the air distribution channel by installing distributors in its path. This will reduce the air pressure as a result of mixing the flow of the drying agent and the aerodynamic impacts that occur when the flow direction changes.

Considering the above, it can be assumed that all technological methods that are used to maintain the quality of agricultural products of plant origin being procured should ensure the highest possible preservation of useful nutrients when choosing rational schemes for supplying and removing a drying agent. Improvement of the existing equipment that is used in the procurement of crop products is important. Moreover, the characteristics of the material as a drying object, the range of equipment produced, the features of modern agricultural production, and the operating modes of the equipment used for active ventilation should be taken into account, thereby reducing possible quality losses of procured products.

CONFLICT OF INTEREST
None.

ACKNOWLEDGEMENTS
None.

FINANCIAL DISCLOSURE
None.

IIOAB JOURNAL
ISSN: 0976-3104

REFERENCES#

[1] Kasyanov GI, Myakinnikova EI, Zanin DE, Zotova LV. [2014] Device for drying agricultural raw materials. Utility model RF patent 146587 MPK A23B7/02, application 2014129987/13, 21.07.2014, publication 10.10.2014.

[2] Musaev FA, Zakharova OA, Torzhkov NI. [2014] Feed and their zootechnical analysis. Laboratory workshop. Publishing house of Ryazan State Agrarian University, Ryazan. RU

[3] Ostrikov AN, Shevtsov SA. [2013] A formalized approach to extreme control of the process of drying vegetable raw materials with superheated steam. Bulletin of the Voronezh State University of Engineering Technologies, 3:7-12.

[4] Shupik MV, Raikhman AYa. [2014] Feeding livestock. Feeding cattle, sheep, goats and horses. Belarusian State Agricultural Academy, Gorki.

[5] Tyurin IYu. [2000] Improving the process of drying hay at a farm. PhD Thesis in technical sciences, Vavilov Saratov State Agrarian University, Saratov.

[6] Tyurin IYu. [2010] Prospects for the development of experimental studies of the drying process. Scientific Review, 5:76-78.

[7] Tyurin IYu. [2012] Improving the process of drying hay. A monograph, Lap Lambert, Germany.

[8] Tyurin IYu, Levchenko GV, Bezrukov NS, Kladov AA. [2017] Opportunities for automating the drying process. Agricultural Scientific Journal, 10:61-63.

[9] Tyurin IYu, Levchenko GV, Timakov DV. [2015] Ways to improve the drying process. Materials of the XV international scientific-practical conference "Modern concepts of scientific research, Moscow, 6-7.

[10] Mirznanii.com. [2020] Role of feed production in the agro-industrial complex. Available from: 〈http://mirznanii.com/a/13538/rol-kormoproizvodstva-v-sisteme-apk〉.

[11] Dugin YuA. [2008] Improvement of technology and development of a rotary-screw threshing apparatus for threshing chickpeas. PhD Thesis in technical sciences, Volgograd State Agricultural Academy, Volgograd.

[12] Timakov DV, Tyurin IYu. [2017] Conditions for improving the technology of drying crop products. Materials of the 30th Mikhailov International Seminar, Saratov State Agrarian University.

[13] Tyurin IYu, Levchenko GV, Makarov SA, Dugin YuA. [2016] Opportunities for improving the drying process. International Research Journal, 1-3(43):13-14.

[14] Tyurin IYu, Telnov MYu, Graf AI, Lishavskii VS. [2013] Assembly for active ventilation of agricultural crops. Pat. RUS 135225 MPK: A01F25/08, applicant and assignee: Vavilov Saratov State Agrarian University, 2013132284/13.

[15] Khazimov KM. [2014] Selection of the polyethylene type as the screen in the solar dryer for drying vegetables. 11th Conference of European Applied Sciences: modern approaches in scientific researches,. 61-68.

[16] Khazimov KM. [2015] Intensification of the drying process of plant products using solar energy. PhD Thesis, Kazakh National Agrarian University, Almaty, Republic of Kazakhstan.

[17] Khazimov KM, Bora GC, Urmashev BA. [2014] Computation of optimal structural and Technical parameters of solar dryer. IJEIT, 4(1):258-268.

[18] Khazimov MZh, Khazimov KM. [2015] Solar energy dryer. Pat. 30006, Applicant and assignee: Kazakh National Agrarian University, Republic of Kazakhstan.

[19] Khazimov MZh, Khazimov ZhM, Ultanova IB, Sagyndykova AD. [2015] Justification of the effectiveness of the use of a shaft type solar dryer for drying fruits and vegetables. Materials of the International scientific practical conference, Accent Graphics Publishing & Communications, Ontario, 6-12.

[20] Ultanova I, Khazimov K, Khazimov M. [2014] Determination of thermal performance the fruits pulp of melons. Agroinžinerija ir energetika, 19:121-128.

[21] Mikaberidze MSh. [2010] Withering tea leaves using infrared ray]. Monography, Akaki Tsereteli State University, Kutaisi, 89(1):22-30.

[22] Mikaberidze MSh, Kintsurashvili KM. [2014] Technology and technological equipment for drying fruits and vegetables. Textbook, Akaki Tsereteli State University, Kutaisi.

[23] Ostrikov AN, Kalashnikov GV, Shevtsov SA. [2014] The main laws of heat and mass transfer in the process of drying plant food raw materials using superheated steam. Izvestiya vuzov. Pishchevaya tekhnologiya, 4:87-92.

[24] Ostrikov AN, Shevtsov SA. [2005] Kaskadnaya sushilka [Cascade dryer]. Pat. 2244230 RF MPK7 F 26 V 17/04, applicant and assignee: Voronezh State University of Engineering Technologies, 2003122380, application 17.07.2003, publication 10.01.2005, Bulletin 1.

[25] Ostrikov AN, Shevtsov SA. [2004] Sushilka [Dryer]. Pat. 2241926 RF MPK7 F 26 V 17/04, applicant and assignee: Voronezh State University of Engineering Technologies, 2003112746, application 29.04.2003, publication 10.12.2004, Bulletin 34.

[26] Ostrikov AN, Shevtsov SA, Stolyarov AN. [2014] Rotornaya sushilka [Rotary dryer]. Pat. 2520752 RF, MPK F 26 V 17/04, applicant and assignee: Voronezh State University of Engineering Technologies, 2013115610/13; application 05.04.2013, publication 27.06.2014, Bulletin 18.

[27] Shevtsov SA, Ostrikov AN. [2014] Technique and technology for drying plant food raw materials. Voronezh State University of Engineering Technologies, Voronezh.

[28] Sivitskii DV, Mukhin AI. [2015] Ways to increase the drying intensity while maintaining the integrity of the dried material. Scientific contribution of young researchers to the preservation of traditions and the development of agro industrial complex, Saint Petersburg State Agrarian University, Saint-Petersburg,

[29] Tiwari GN. [2008] Solar energy. Fundamentals, Design, Modelling and Applications, Alpha science International, Ltd, India.

[30] Shhitov SV, Samarina YuR, Krasnoshhyokova TA, Sharvadze RL, Kapustina NA. [2016] Substantiation of design-operating conditions of infrared drying unit. Far East Agrarian Bulletin, 4(40):183-190.

[31] Babaev GG, Matyakubova PM, Nasimkhanov LN. [2016] Study of the infrared method of drying grain and granular materials. Molodoi uchenyi [Young scientist], 14(118):116-118.

[32] Mehanik-ua.ru. [2020] Justification of parameters and operating modes of infrared drying devices for drying fruit and vegetable products in farms. Available from: 〈https://mehanik-ua.ru/sbornik-statej/1626-obosnovanie-parametrov-i-rezhimov-raboty-infrakrasnykh-sushilnykh

[33] Lapshov MO. [2018] The use of irradiation plants for IR heating and drying in agriculture. Scientific and practical electronic journal of the Alley of Science, 8(24):1-5.

English translations of the original references are presented.